Genetic Mapping and Sequence Analysis of Candidate Genes Causing Non-Syndromic Polydactyly

QUAID-I-AZAM UNIVERSITY

ISLAMABAD

by

Romana Liaqat

Department of Biochemistry
Faculty of Biological Sciences
Quaid-i-Azam University
Islamabad, Pakistan
2019

Genetic Mapping and Sequence Analysis of Candidate Genes Causing Non-Syndromic Polydactyly

A thesis submitted in the partial fulfillment of the
requirements for the degree of
Master of Philosophy

in

Biochemistry/Molecular Biology

by

Romana Liaqat

Department of Biochemistry
Faculty of Biological Sciences
Quaid-i-Azam University
Islamabad, Pakistan
2019

بِسْمِ اللَّهِ الرَّحْمَٰنِ الرَّحِيمِ

In the Name of ALLAH, the Most
gracious, the Most Merciful.

This Thesis is Dedicated
To
My Loving Parents and my elder
sister
For their endless love, support,
encouragement and prayers

Declaration

I hereby declared that the work presented in this thesis is my own effort and hard work; it is written and composed by me. No part of this thesis has been previously published or presented for any other degree or certificate.

Romana Liaqat

CERTIFICATE

This thesis, submitted by **Ms. Romana Liaqat** to the Department of Biochemistry, Faculty of Biological Sciences, Quaid-i-Azam University, Islamabad, Pakistan, is accepted in its present form as satisfying the thesis requirement for the Degree of Master of Philosophy in Biochemistry/Molecular Biology.

Supervisor:

_____
Dr. Wasim Ahmad
Professor

External Examinar:

_____
Dr. Attya Bhatti
Associate Professor
National University of Science & Technology
(NUST) H-12, Islamabad.

Chairman:

_____
Dr. Muhammad Rashid Khan
Professor

Dated: April 24, 2019

List of Contents

ACKNOWLEDGEMENTS

All praises and glories to **Almighty "ALLAH"** who says in the Holy Quran, "And your Lord is the most gracious who taught by the pen, taught man (those things) which he did not know". Countless Darood on Prophet **HAZRAT MUHAMMAD (Sall-Allah-Ho-Alaihay-Wa-Aalayhi-Wasallam),** who showed the path of knowledge to mankind and gave the lesson of seeking knowledge from cradle to grave.

I am greatly honored to pay my deep gratitude to the most learned, perfectionist and considerate supervisor **Prof. Emeritus Dr. Wasim Ahmad**, Department of Biochemistry, Faculty of Biological Sciences, Quaid-i-Azam University Islamabad, under whose inspiring guidance and encouragements this research work was carried out. I'm also thankful to Chairperson, Department of Biochemistry,**Prof Dr. Muhammad Rashid Khan** for dedication to thrive these research activities in the department.

I would like to acknowledge my worthy PhD seniors **Dr. Khadim Shah, Dr Muhammad Umair, Dr. Asmat Marwat, Dr. Farooq Ahmad, Amir Hayat, Pashmina Wiqar Shah, Abdullah, Laila Akbar, Muhammad Bilal, Maryum Khan** for their cooperation, suggestions and nice company during my research work, which is precious to me in all regards because without their help and cooperation in my research would be really difficult.

I also acknowledge the friendly and cooperative attitude of my lab fellows **Warda Nawal, Qari Ijaz Ahmed, Qari Aziz-ur-Rehman,** and **Maria Hayat,** for their cooperation and respect that they gave me in the lab during research.

I present heartiest thanks to my dear roommate and my friend **Asiya Essa** for adoring me and filling every moment of my hostel life with such joy that I never felt any moment of sadness. My friend **Shaheen Wazir** was always supporting and encouraging me with her best wishes, prayers and love. My friend **Maria Aman**, the time spent with her can never be erased from my memories. I'm also thankful to my teachers for their valuable suggestion specially **Dr. Muhammad Iqbal, Dr. Syed Badshah Mehsud** and **RizwanUllah Khan.**

It's utterly true that "Behind every successful girl there is an open minded father who trusted his daughter and not the society", no words can express my deepest gratitude and feelings to my dearest father **Dr.Liaqat Ali Mehsud** whose firm dedication, inbuilt confidence and untiring efforts, they have done to adorn me with the jewels of education. I also owe deepest gratitude to my brothers **Dr. Raiz ul- Din Mehsud,** and my dearest **Zain ul abidin Mehsud**. and sisters Specially Mrs. **Zahida Liaqat,** her moral support, love and prayers throughout my studies. I owe you my whole life, my dear **mother**, May Allah have mercy upon you and bless you with Jannah in the world hereafter.

Additionally I convey my heartiest thanks to the departmental clerical staff especially **Mr.Noor Habib**, **Mr. Tariq, Mr. Fayyaz**, **Mr. Shehzad,** and **Mr. Saeed** for their services towards students.

Last but not the least, I thank all the diseased families that were involved in this research study for their cooperation and participation and their efforts for the completion of my thesis.

RomanaLiaqat

List of Figures

Figure 3.38	Allelic arrangements attained with respective STS markers on chromosome 8q22.1 from candidate gene *FAM92A*.	74
Figure 3.39	Allelic arrangements attained with respective STS markers at chromosome 13q13.3-q21.2.	75
Figure 3.40	Allelic arrangements attained with respective STS markers at chromosome 13q21-q32.	76
Figure 3.41	Allelic arrangements attained with respective STS markers at chromosome locus 19p13.1-13.2.	77
Figure 3.42	Sequencing chromatogram of *ZRS/SHH* with novel point mutation	78

	List of Tables	
Page No	**Title**	**Page No**
Table 2.1	Composition of Solutions Used in Standard Phenol-Chloroform Method	19
Table 2.2	Composition of Solutions Used for Agarose Gel Electrophoresis	21
Table 2.3	Conditions used for performing PCR.	23
Table 2.4	Composition of Chemical used for Polyacrylamide Gel Electrophoresis	24
Table 2.5	Thermo-cycling conditions used in Asymmetric sequencing PCR	26
Table 2.6	Microsatellite Marker Used for Mapping Polydactyly	31
Table 2.7	List of GLI 3 Primer sequences	35
Table 2.8	List of Primers used for Sanger Sequencing of ZRS	36

List of Abbreviations

Symbols	Abbreviations
%	Percentage
AER	apical ectodermal ridge
AP	anterior posterior
ATF	Activating Transcription Factor
BBS	Bardet-Biedl Syndrome
BDA1	brachydactyly type A1
BDC	Brachydactyly type C
BMP	Bone morphogenetic protein
bp	Base pair
cM	centiMorgan
C- Terminus	Carboxyl terminus
CP	Cross Polydactyly
CTGF	Connective tissue growth factor Cysteine
Cys	Cysteine
^{0}C	Centigrade
DNA	Deoxyribonucleic Acid
RNA	Ribonucleic acid
Del	Deletion
dNTPs	Deoxynucleotide triphosphate
DV	Dorso-ventral
EC	Extra cellular domain

Page Cont.

AER	apical ectodermal ridge
AP	anterior posterior
TE	Tris- EDTA
TEMED	N, N, N', N' Tetramethylethylenediamine
Tm	Annealing temperature
UV	Ultraviolet
v/v	Volume by volume
μg	Microgram
μl	Microliter
EDTA	Ethylene-Diamine-tetra-acetic acid
EMT	Epithelial Mesenchymal Transition
EN-1	engrailed-1
EPS8L3	Epidermal growth factor receptor kinase substrate 8-like protein3
EVC	Ellis–van Creveld
FGF	fibroblast growth factor
FGFs	fibroblast growth factors
FOXN1	Fork head box protein N1
g	Gram
GLI3	Glioma-associated oncogene 3
Grem1	Gremlin 1
HCl	Hydrochloric acid
IHH	Indian hedgehog

Page Cont.

LPM	lateral plate mesoderm
PAP	postaxial polydactyly
PD	proximal to distal
PFR	phalanx-forming region
PPD	preaxial polydactyly
PTHLH	parathyroid hormone like hormone
SHH	Sonic hedgehog
TBX	T-Box gene
TGF-β	Transforming growth factor beta
TPT	Triphalangeal thumb polydactyly
ZPA	zone of polarizing activity
ZNF141	Zinc finger protein 141

Abstract

Abstract

Several signaling pathways, by involving large number of proteins, play important roles in development of human limbs. Disturbances in the functions of the protein encoding genes lead to result in different types of congenital limb deformities. These anomalies occur either as an isolated malformation of the hands/feet or as a part of complex syndrome. In humans, polydactyly is the most frequently observed congenital hand and feet malformation. Major type of non-syndromic forms of polydactyly is classified into pre-axial, postaxial and central type polydactyly.

In the present study, four consanguineous families (A, B, C, D) segregating polydactyly were recruited from different remote regions of the country. Pedigree sketches showed segregation of the disorder in three families (A-C) followed autosomal recessive mode of inheritance. Family D, on the other hand, showed autosomal dominant mode of inheritance.

Linkage in the family A-C was searched by typing microsatellite markers linked to several candidate genes involved in causing polydactyly. Analysis of the haplotypes, constructed from the typed markers, however excluded the families from linkage to the tested genes. Sequencing of two candidate genes (*GLI3, ZRS/SHH*) in affected and unaffected members revealed a heterozygous variant (c.1034 + 182 T>C) in enhancer sequences located in intron 5 of the *LMBR1*. The variant is predicted to affect the expression of the *LMBR1* leading to autopod anomalies.

The present study will not only be helpful in identifying additional genes involved in human limb development but also facilitate prenatal diagnosis and genetic counseling of the families showing polydactyly features.

Chapter 1
INTRODUCTION

Abstract

Several signaling pathways, by involving large number of proteins, play important roles in development of human limbs. Disturbances in the functions of the protein encoding genes lead to result in different types of congenital limb deformities. These anomalies occur either as an isolated malformation of the hands/feet or as a part of complex syndrome. In humans, polydactyly is the most frequently observed congenital hand and feet malformation. Major type of non-syndromic forms of polydactyly is classified into pre-axial, postaxial and central type polydactyly.

In the present study, four consanguineous families (A, B, C, D) segregating polydactyly were recruited from different remote regions of the country. Pedigree sketches showed segregation of the disorder in three families (A-C) followed autosomal recessive mode of inheritance. Family D, on the other hand, showed autosomal dominant mode of inheritance.

Linkage in the family A-C was searched by typing microsatellite markers linked to several candidate genes involved in causing polydactyly. Analysis of the haplotypes, constructed from the typed markers, however excluded the families from linkage to the tested genes. Sequencing of two candidate genes (*GLI3, ZRS/SHH*) in affected and unaffected members revealed a heterozygous variant (c.423+4695 and g.101537T>C in intron 5 of *LMBR1* (*ZRS/SHH* at 182 T>C) in enhancer sequences located in intron 5 of the *LMBR1*. The variant is predicted to affect the expression of the *LMBR1* leading to autopod anomalies.

The present study will not only be helpful in identifying additional genes involved in human limb development but also facilitate prenatal diagnosis and genetic counseling of the families showing polydactyly features.

gives rise to the limb skeletal structure (appendicular skeleton), the sternum (axial skeleton) and the non-skeletal elements. The paraxial mesoderm gives rise to somites forming the axial skeleton, such as ribs and vertebrae (Sauka-Spengler, and Bronner-Fraser, 2008; Limura *et al.*, 2009).

Skeletal Patterning

During the period of endochondral bone formation, limb skeleton build up from cartilage anlagen. It begins with the chondrocytes progenitors which then develop into a cartilage template that is eventually substituted by bones. The crucial steps in establishing limb skeletal pattern 'patterning' take place throughout the formation of cartilaginous anlagen (Tickle, 2003). Skeletal patterning, condensation and differentiation of mesenchymal cells (MSCs) into chondrocytes (cartilage formation), osteoblasts (bone formation), osteoclasts, and bone remodeling is under tight control of several cytokines, growth factors and intercellular signaling pathways including Wingless/Integrated (*Wnt*), Sonic hedgehog (*SHH*), Indian hedgehog (*IHH*), fibroblast growth factor (*FGF*), *Notch*, *TGF-β*, and *BMPs*. Genetic variations in cytokines and growth factors lead to inherited skeletal disorders (Lefebvre and Bhattaram, 2010). During the skeletal patterning and remodeling the size, shape, number and the skeletal primordial in correct relationship to one another are defined. Different skeletal elements like axial, craniofacial and appendicular skeleton are formed during the skeletal patterning process in organized way (Mariani and Martin, 2003).

Limb Development

The development of limb in vertebrates is controlled by the genetic processes which are impenetrable and still not fully understood. Experimental studies of the molecular genetics of human limb development is theorizing and manipulating the genetic interactions in them. There are three principle zones for the development of limbs that is the proximal stylopod, Zeugopod and the distal autopod (Berham *et al.*, 2008).

Initiation of Limbs

The limb bud originates from the edge of the embryo that is, the lateral plate mesoderm (LPM) which is covered by a layer of ectoderm. It has lineages for all

types of limb tissues except muscles. Muscles progenitors initiate from somites and rapidly migrate to embryonic limb bud. The skeletal element elaborates when the tissue progenitors differentiate and the limb bud grows towards the distal side. The limb bud when grows towards the distal side, the varied tissue progenitors differentiate and establish the elaborated pattern of skeletal elements (Mundlos and Horn, 2014).

The *HOX* gene plays a fundamental role during embryonic development. It generates the morphological diversity together with the body axis and determines the position of the limb buds genetically (Kmita and Duboule, 2003). When the position of the limb is decided than a series of interactions between the epithelial-to-mesenchymal and the lateral plate mesoderm, ectoderm is established. In this event the establishment of apical ectodermal ridge (AER), an epithelial thickened structure from limb ectoderm, occurs which facilitate the distal margins of the limb bud to its posterior tip from its anterior side and is dorsoventrally located along the border of the limb bud (Capdevila and Belmonte, 2001). Several studies have revealed that a number of molecules expressed in specific domains either in dorsal or ventral ectoderm are involved in limb developmental process, some example being *WNT7A*, Radical fringe (*RFN*), Engrailed-1 *(EN-1)* and *TGF-β/BMP* (Capdevila and Belmonte, 2001).

Limbs Patterning

After the development of limb bud the undifferentiated mesenchyme is targeted by a series of signaling to determine the morphology of skeletal elements. The AER (apical ectodermal plate), the zone of polarizing activity (ZPA), and the dorsal ectoderm plays a key role to control the limbs proximal to distal outgrowth, anterior posterior (AP) patterning and establishes dorso-ventral polarity, respectively (Mundlos and Horn, 2014). The limb buds have mesoderm cells, homogenous mass covered with a layer of ectoderm. The initial mark of patterning is in the form of a thin epithelial thickening at the limb bud proximal tip which is known as the Apical Ectodermal Ridge (Lodder, 2009). The AER is important for proximal to distal patterning and it is revealed that when the AER in chick wings are removed, the wings become truncated (Niswander, 2003). The cell death in the mesenchyme occurs very sharply after removal of the AER (Saunders, 1948; Summerbell, 1974). These

cells can survive if fibroblast growth factors (FGFs) are applied exogenously. AER promote proliferation of mesodermal cells, stops apoptotic events by providing *FGF* signaling to the mesoderm cells (Mundlos and Horn, 2014). *FGF10* expression which is required for maintaining *FGF8* expression in the limb mesenchyme is induced by the AER expressed *FGFs* (*FGF 8, 9, 17*). Thus *FGF8* and *FGF10* establish epithelial-mesenchymal positive feedback loop during limb growth (Benazet and Zeller, 2009). During limb development, abnormalities in the AER maintenance lead to abnormal phenotypes including split-hand/foot syndromes as a results of *TP63* mutations in, whose expression is vital for AER maintenance (Lanakiev *et al.*, 2000). A cell colony termed as the zone of polarizing activity (ZPA), is localized in the posterior limb bud mesenchyme that shows posture activity (Rubin and Saunders, 1972). The molecular basis of ZPA was discovered when Sonic hedgehog (*Shh*) was proposed to be the diffusible morphogen responsible for polarizing activity (Yang *et al.*, 1997). Another gene reported was Glioma-associated oncogene 3 (*GLI3*) which has two isoforms, one with active full length *GLI3* (*GLI3F*) and repressor truncated *GLI3* (*GLI3R*). SHH signaling promotes the expression of *GLI3F* in posterior mesenchyme while absence of *SHH* signaling leads to the production of *GLI3R* (Zeller *et al.*, 2009).The importance of *GLI3* and *SHH* during vertebral limb growth was discovered in mouse by gene inactivation; *SHH* mutant mice had only one rudimentary digit while all other digits were absent, on the other hand *GLI3* mutant mice verify polydactyly. *SHH* and *GLI3* mutations in human leads to different limb anomalies including preaxial or postaxial polydactyly or even severe conditions like acheriopodia (Anderson *et al.*, 2012). *SHH* play key role in AP patterning, maintains limb bud proliferation and expands the digit forming field (Zeller *et al.*, 2009). *SHH, GLI3* and other regulators promote digit number and identity. In this context a BMP (bone morphogenetic protein) signaling gradient was also suggested as a mediator while genetic analysis of mouse did not prove its role. It was shown that patterning information in chicks are stored in the interdigital mesenchyme. Signals to the growing phalanges are thought to be the signals from the interdigital mesenchyme, which provide them information necessary for reaching its final length (Zeller *et al.*, 2009). Dorso-ventral patterning is mediated by *LMX-1* (LIM homeobox transcription factor-1) in the dorsal mesenchyme with subsequent expression of *WNT-7A* in the dorsal ectoderm and engrailed-1(*EN-1*) in the ventral ectoderm. In the ventral ectoderm, *EN-1* inhibits the

WNT7A expression (Yang and Niswander, 1995; Bell *et al.*, 1998). Acting as a morphogen *WNT7A* diffuses to the dorsal mesoderm and induces expression of the *LMX1B* (transcriptional factor). In the limb bud mesenchyme, *LMX1B* is considered as a key regulator of dorsal patterning. *LMX1B* mutation in human result in a syndrome characterized with a defect in dorsal to ventral (DV) patterning of the limb, which is known as nail-patella syndrome (Dreyer *et al.*, 1998).

Signaling Pathways Involved in Limb Patterning

This is innate that AER, dorsal ectoderm, and ZPA are the centers of signaling and have strong coordination in their functions. It is perceived that AER removal result in cell death in the underlying mesenchyme and leads to loss of *SHH* expression. Interestingly, *FGF4* could reimburse this function of the AER. Similarly, *SHH* actively controls *FGF4* expression in the AER, thus both (*SHH* and *FGF4*) molecules form a positive feedback loop. This feedback loop is a best example of a signal relay in epithelial-to-mesenchymal communication: *SHH* actively controls the Gremlin 1 (*Grem1*) expression, which is a BMP inhibitor. Taken together, *GREM1* inhibits BMP action, which has a negative effect on the AER (Benazet and Zeller, 2009). *WNT7A* is required to replace the removed ectoderm while *SHH* is expressed in the dorsal mesoderm. In mammals this function is highly conserved, thus there is quite decrease in *SHH* expression by the inactivation of *WNT7A* as a result the posterior digit is lost (Barrow *et al.*, 2003)

Limb Identity

The expression of *HOX* gene in the limbs is considered for the alignment of hind limb and forelimbs identity expressed by the T-Box gene (*TBX4* and *TBX5*) in chicks and performed a very innovative role in limbs identity but this phenomena is not sustained in all animal model by the geneticist specially in mouse embryo (Bruneau *et al.*, 2001, Duboc and Logan, 2011). Expression of *PITX1* by *TBXX4* and mis-expression of *PITX1* in the fore limbs of chicks led to the development of hind limb characteristics. *PITX1* mutations in humans were detected in two syndromes that are both specific to hind limbs and lead to morphological variations in the forelimbs towards hind limb-like structures. *PITX1* mutation also causes clubfoot and various other limbs irregularities (MIM 119800) and patients also revealed polydactyly or tibial

hemimelia but normal upper extremities. On the other hand, genomic rearrangements upstream of *PITX1* were associated with Liebenberg syndrome (MIM 186550), having upper limb irregularities symptomatic of a hind-limb-like morphology (Spielmann *et al.*, 2012).

Skeletal Dysplasia

Skeletal dysplasia or Osteochondrodysplasias are phenotypically and genotypically heterogeneous group of disorders affecting the growth of bone and cartilage growth (Namba, 2010). It has significant effects on muscles, tendon and ligaments. It is frequently related with abnormalities of linear skeleton and result from teratogen exposure and imprinting errors (Karkow and Rimoin, 2010). Mutation in the signaling pathways of metabolism, homeostasis, growth factors or transcription factors, macromolecules degradation are major cause of skeletal dysplasia (Ullah et al., 2018).

Classification of Skeletal Disorders

Nomenclature and classification of Osteochondrodysplasias is termed as "taxonomy". When the Dysostoses is incorporated into the nomenclature it is called as "nosology" (Mundlos and Olsen, 1997; Hall, 2002). In past from 1977 to 1997 several revisions for classifying the nosology (skeletal dysplasia) were published, to categorize different skeletal disorders on the basis of clinical diagnosis, metabolism and radiology. The list of genetic disorders mentioned in nosology helps to diagnose and delineate variants or newly recognized genetic disorder (Warman *et al.*, 2011). There are 436 disorders, classified into 42 groups. The classification was carried out on the basis of involvement of 364 different genes, in establishing molecular pathways, genetic, radiographic criteria and role of biochemical were defined as the cause of these disorders. Recently new revision of ISDS (International Skeletal Dysplasia Society) was carried out to amend the nosology and also include recently identified genes/loci and the disorders identified with new pathological and molecular concept.

Limb Deformities

The growth and development of the limbs involve several genetic pathways and disruption of these genetic pathways escort to variety of anomalies in size, figure and formation of the limbs collectively known as congenital limb deformities. Limb deformities involve abnormal fingers stature in hands/feet, uneven number of the digits or the deviation of central rays of the autopods. Congenital limb malformations rate is 1/500 in live births for upper limbs (Furniss *et al.*, 2009). In the present dissertations we focused on non syndromic polydactyly.

Polydactyly

Polydactyly comes out of "poly, means many and dactylos meaning digits". It is most common hereditary limb anomaly also known as hyperdactyly or hexadactyly (Ullah et al., 2019). The term polydactyly is used to describe the existence of supernumerary digits, toes/digital duplication. This situation was described as "superfluous fingers" in the 16th century by Ambrose Parey (Bell et al., 1953) This anomaly is immediately observable at birth and shows a broad spectrum of phenotypes ranging from inclusive to partial duplication. Generally its prevalence found as 1.6-10.7/1000 in the population. The proportion of male affected with polydactyly are twice as compared to females (Mellin, 1963; Castilla *et al.*, 1973). There is high tendency for the involvement of right hand than the left one, upper limbs than the lower limbs, and left foot than the right one is reported in literature (Temtamy and McKusick., 1978; Castilla *et al.*, 1973; Malik *et al.*, 2014, Umair *et al.*, 2018).

Classification of Polydactyly

Polydactyly is classified into two broad categories such as syndromic and non-syndromic preaxial, postaxial, and complex polydactyly.

Syndromic Polydactyly

There are 221 syndromes with polydactyly and 120 with Oligodactyly are listed in London Dysmorphology Database (Simon *et al.*, 1999).The commonly seen syndromes with digit abnormalities are Bardet Biedl syndrome, Ectrodactyly–Ectodermal-Dysplasia- Clefting syndrome (EEC), Greig Syndrome, Cornelia de

(Temtamy and McKusick, 1978). It shows autosomal dominant inheritance pattern. The normal digit deviated at varying degree towards the ulnar side or radial deviation may take place in the extra digit (Gillessen-Kaesbach, 1991; Perez-Lopez *et al.*, 2018).

Preaxial Polydactyly type 4

This is also known as the Polysyndactyly (MIM 174700) as the third and fourth fingers syndactyly may present rarely but the metacarpal is tibially deviated and short of first toe, whereas the thumb is broad, bifid, duplicated mildly or the distal phalanx show radial deviation (Malik, 2012; Burger *et al.*, 2018). For this type of polydactyly word "crossed polydactyl" or "CP" also used as post axial and preaxial both phenotypes may appear in single case but with a difference in feet and hand axis of extra length. CP1 have postaxial polydactyly in hand and preaxial in feet while in CP 2 replacement takes place as postaxial in feet and preaxial in hand Polydactyly is reported (Temtamy and McKusick, 1978). Mutations in *GLI3* and in *SHH/ZRS* have been associated with this type of polydactyly and up till now 216 mutations are reported (Perez-Lopez *et al.*, 2018, Umair *et al.*, 2018).

Preaxial Polydactyly type 5 or Hallux Polydactyly

Preaxial polydactyly or Hallux Polydactyly (MIM 601759) has peculiar features of polydactyly with duplication of digits. It was mapped at chromosome 2q31.1-31.2 with 3.4 Mb interstitial deletions but the causative gene is still not identified and still under studies (Castilla *et al.*, 1973; Shwabi and Mundlos, 2004). This occurs more commonly in right foot and the incidence of Hallux polydactyly in male is more reported than female (Orioli and Castilla, 1999).

Complex type of Polydactyly

This type of polydactyly is classified separately because it possess different clinical in muscles mass of hand features from Preaxial Polydactyly (PPD) and Postaxial Polydactyly (PAP).

Central Polydactyly

Central polydactyly also called Mesoaxial polydactyly has hidden duplication like second digit in middle part of hand or manifest syndactyly, present as mass of tissues, however it is not necessary that all types are hidden. It is frequently bilateral and duplicated in fourth index digit of hand (Temtamy and McKusick, 1978; Winter and Tickle, 1993; Graham and Ress, 1998; Lange and Müller, 2017).

Haas Type Polysyndactyly

This type of polydactyly is also classified as Type 5 syndactyly. In this type, the web fingers are fused cutaneous, give a cup shaped appearance and have an extra projection like PPD and PAP (Malik, 2012). The movement is restricted due to complete syndactyly. It is certified as a genetically heterogeneous anomaly. The causative mutations in genes to cause Haas type polydactyly are identified as *GLI3* and *ZRS* (Lohan *et al.*, 2014)

Mirror-Image Polydactyly

This type of deformity (MIM135750), possesses exchange of anterior digits and duplication in posterior digits occur. The central digits that are the little finger with hallux/thumb, middle finger, little finger along with ring finger is absent. Laurin-sandrow syndrome (MIM 135750) also possesses such phenotypes and considered as the part of this abnormality. There are also cases reported in literature with complete duplication of fingers 10 digits from left and nine from right and give a bilateral pattern (Martin *et al.*, 1993; Temtamy and McKusick, 1978). This is usually autosomal dominantly inherited and the mutation identified on causative genes are PITX1 (MIM 602149), there are 17 mutations identified at this gene and MIPOL1 (MIM 606850) was mapped at chromosome locus 14q13 (Kondoh *et al.*, 2002, Klopocki *et al.*, 2012).

followed by separation of upper most layer (containing DNA) in another eppendorf tube.

- Subsequently DNA sample in new eppendorf tube was precipitated after adding 500 µl of Isopropanol (chilled)and 66 µl of 3M sodium acetate andtube was inverted many times so as the DNA precipitation can occur.

- To get the pellet of precipitated DNA again centrifugation was performed for 13000 rpm/10 mint, and supernatant was discarded.

- DNA pellet was then dissolved in 200 µl of 70% ethanol (chilled) and allowed to centrifuge for 13000 rpm/7 minutes. .

- After this ethanol was carefully discarded and the nuclear pellet obtained was dried inside the vacuum concentrator at 45°C for 15 minutes. The pellet (DNA) obtained was diluted by adding 120-180 µl of TE buffer (Tris-EDTA) by incubating overnight at 37 °C.

- On the next day, after the pellet was completely dissolved in TE buffer, the DNA was checked on 1% agarose gel and stock DNA was stored at 4°C.

Table 2.1: Composition of Solutions Used in Standard Phenol-Chloroform Method

Solution used	Composition	Concentration
Solution A	Sucrose	0.32 M
	Tris(pH 7.5)	10mM
	MgCl$_2$	5mM
	Triton X-100	1%(v/v)
Solution B	Tris (7.5)	10mM
	NaCl$_2$	400mM
	EDTA(pH)	2mM
Solution C	Phenol (100%)	
Solution D	Chloroform	24:1 by volume
	Isoamylacohol	
SDS 20%	SDS + Distilled Water	10g in 50ml

Commercially Available DNA Extraction Kit

Commercially available kit (QIAGEN GmbH, QIAGEN Strsse 1, and 40724 Hilden, Germany) was used for DNA extraction using manufacturer's instructions.

- 200 µl of blood was mixed with equal amount of lysis buffer and 18 µl proteinase K (9.8 mg/mL) in an eppendrof tube, further mixed gently by vortexing for 5-10 seconds followed by incubation in water bath at 65°C for 10 minutes.

- The mixture was mixed with 200 µl chilled ethanol (96-100%) and centrifuged at 7,000 rpm/60 seconds and residual was discarded. These steps were repeated and column containing the flow-through liquid was run at 13,000 rpm/2 minutes to give an empty spin.

- The DNA was eluted by using 80-100 µl Tris-EDTA into the column after keeping it in a new tube at 25°C for 5 minutes.

- Centrifugation was performed at the highest rpm for 2-3 minutes and the DNA was obtained and stored.

Agarose Gel Electrophoresis

Extracted DNA from blood was analyzed on 1% agarose gel for quantitative and qualitative analysis by visualizing the gel bands. Agarose gel was prepared according to the size of the sample. Usually for DNA quantification 1% agarose gel is prepared. Chemicals used and their composition are given in Table 2.2. For 1% agarose gel preparation containing total volume of 100 ml, 1 g of agarose was added into conical flask and then 10 ml of 10X TBE buffer was poured and 90 ml of distilled water. The agarose in solution was dissolved by heating at high temperature in an oven for 60-65 seconds. When agarose was completely dissolved, then 6 µl of EtBr was added in the gel solution and by gently shaking the solution was mixed and poured into gel tank and kept for half an hour at 25°C for proper polymerization. 4 µl of loading dye was mixed with 4 µl of extracted DNA and loaded into the wells followed by electrophoresis at 100 volts for 25-30 minutes in running buffer (1X TBE). The DNA bands were stained with EtBr (10 mg/ml) and visualized by modern gel doc system (FluorChem FC3 protein simple 3001 Orchard Parkway San Jose, California, 95134 USA).

Table 2.2: Composition of Solutions Used for Agarose Gel Electrophoresis

Chemicals	Composition
Agarose	As required
Ethidium bromide	0.5 µg/ml final concentrations
Gel Loading dye	0.25% bromophenol blue
	40% Sucrose
10X (TBE buffer)	0.032 M EDTA (pH 8.3) 0.025 M Borate 0.89 M Tris
1X (TBE buffer)	EDTA (pH 8.3) 0.032M Borate 0.025 M Tris 0.89 M

DNA Quantification and Dilution

After Agarose gel electrophoresis the quantity of DNA was measured by Nano drop and also the DNA quantification was performed by using Gene Ray UV-Photometer (Biometra®, Germany). DNA was diluted to 40ng/µl by adding PCR water.

Homozygosity MappingUsing Microsatellite Markers

Homozygosity mapping using microsatellite markers (Table 2.7) was applied to establish linkage in the family. Homozygous pattern of alleles showed by affected and heterozygous in normal individuals were hypothesized to establish linkage in the family to the locus/gene. On the other side, heterozygous pattern of alleles showed by normal and affected individuals was considered to exclude the family from linkage to that specific locus.

Polymerase Chain Reaction (PCR)

To check the homozygosity through linkage or mapping, simple sequence repeating units (SSR) which are also known as microsatellite markers were amplified through

PCR. The reaction was carried out in PCR tubes (200 µl) and total volume of PCR mixture for reaction obtained was 25 µl, by mixing the following chemicals:

❖ PCR reaction was performed in 200 µl properly labeled PCR tubes containing 25 µl total reaction mixture.

❖ First 1-2 µl of genomic DNA (template DNA) was loaded in 200 µl PCR tubes, and then 23 µl of master mix was added to PCR tubes. Master mix was prepared by adding 2.5 µl of PCR reaction buffer,2 µl of $MgCl_2$, 0.5 µl of dNTPs mixture, 0.3 µl of forward and reverse marker (STS), 0.3 µl of 1unit Taq DNA polymerase and 17.3 µl of PCR water in an eppendrof tube. Before loading into the PCR tubes already containing 2.5 µl of DNA template,

❖ The mixture was given short spin (4,000 rpm/10 seconds) for gentle integration and placed in a thermocycler.

❖ PCR reaction was performed by means of PCR system (9600 and T3 Thermocycler).

PCR Amplification Profiles

The amplification parameters were optimized for individual primer. Standard amplification conditions are given in table 2.3.

Tables 2.3: Conditions Used for Performing PCR

Steps	Sub Cycles	Temperature	Time (Minutes)
Initial Denaturation		96°C	5-7
40 PCR cycles	1. Denaturation	96°C	1
	2. Primer annealing	52 – 63°C	1
	3. Primer Extension	72°C	1
Final Extension		72°C	10

Polyacrylamide Gel Electrophoresis (PAGE)

The amplified PCR products wereanalyzed, for the genotype banding pattern, on 8% polyacrylamide gel electrophoresis. Composition and concentration of 8% polyacrylamide gel are mentioned in Table 2.4.

1) The said mixture poured in a way that the glass plates were separated by two spacers and clips about 1.5mm apart.

2) By inserting the combs, proper wells were provided and left for an hour at 25 °Cfor proper solidification.

3) Loading Dye plus PCR product obtained was taken in equal amount of 5 μl and loaded in wells. It was left forthree hours vertical gel electrophoresis in a glass tank at 140 volts.After sufficient running, with loading dye at the edge of gel approximately, gel was taken and stained with ethidium bromide (0.5 μg/ml) for UV visualization and finally digital camera was used to capture images.

Table 2.4: Composition of Solutions used for Polyacrylamide Gel Electrophoresis

Chemical Used	Composition andConcentration	Amount per gel
30% Acrylamide	29 g of polyacrylamide + 1g of N'N' Methylenebisacrylamide (29:1)	13.5
10X Tris-Borate EDTA	Tris 0.89M Borate 0.89M EDTA 0.02M	5
10% APS	Aluminum persulphate	0.35
TEMED	N'N'- tetra Methyl Ethylene Diamine	0.025
Nucleases free Water		31.125
Total volume		50ml

Sanger Sequencing of Genomic DNA

Based on previous association of *ZRS/SHH* with dominant polydactyly, the same gene was sequenced in DNA of affected and unaffected individuals using gene specific primers. For exons amplification two types of PCRs were performed.

First Sequencing PCR or Pre-sequencing PCR including

For the amplification of *ZRS/SHH*, the reaction mixture was carried out in 200μl of PCR tube and total 50 μl reaction mixture was prepared. 5 μl of PCR buffer together with 2.5 μl of template DNA plus 2.5 μl each of forward and reverse primer and 3μl of MgCl$_2$ including 1 μl of dNTPs as well as 0.7 μl of Taq polymerase and 31.8 μl of PCR water.

The PCR tube was congregated in thermocycler and the reaction was carried out by using same conditions as previously performed. The product (exons amplification) verification was confirmed by running on 2% agarose gel in 1X TBE (running buffer) and the samples were loaded in such a way that 3 μl PCR product with 3 μl bromophenol blue was loaded into the wells and run for 35 min at 110 volts horizontally.

First Purification of Amplified PCR products

When the amplification was confirmed on 2% agarose gel by visualizing gel bands the PCR products was purify by using Axygen Biosciences PCR Cleanup Kit (Invitrogen). Following steps were carried out during purification

> ➢ 120 μl of binding buffer solution (buffer A) was added to the PCR tube containing amplified PCR product and mixed thoroughly by vortexing.

> ➢ Mixtures were poured in column, assembled in 2 ml collection tube and centrifugation was carried o u t a t 13000rpm/1min. Afterward the flow-through liquid was discarded.

> ➢ The column was washed with 500ul ethanol-added washing buffer twice followed by centrifugation at 13000 rpm for 1 mint.

- ➤ The waste collected in the collection tube was discarded and column was placed again in the tube and centrifugation was performed at 13,000 rpm for 2 mints to remove any residual.

- ➤ Thecolumn was transferred to a fresh labeled collection tube and elution buffer (25 μl) kept at 70°C was added.

- ➤ After 7 mints incubation, the centrifugation was performed (13,000rpm/3 min) and the purified product was finally collected in an eppendorf tube.

- ➤ The purified product was evaluated by running on 2% agarose gel. 3 μl of DNA was mixed with 3μl bromophenol blue (loading dye) and loaded onto the gel.

Second Sequencing PCR or Asymmetric PCR

The pre-sequencing products were further preceded to cycle sequencing. 10 μl reaction mixture in a PCR tube was prepared by adding 1 μl of DNA template, Each forward and reverse primer as well as 1 μl of 5x sequencing Buffer together with 1 μl Ready reaction mixture (RR) plus 5μl of PCR water was added and the reaction was processed. The thermo-cycling protocol applied is given in following table 2.5.

Table 2.5: Thermo-cycling conditions used in Asymmetric sequencing PCR

Steps	Sub Cycles	Temperature	Time
Initial Denaturation	Once	96°C	1 minute
30 PCR Cycles	Denaturation	96°C	25- 30 seconds
	Primer Annealing	50-60°C	30 seconds
	Extension	65°C	4 minutes
Final Extension	Once	72°C	10 minutes

Second Purification of Sequencing PCR Product

The sequencing PCR products were purified by the ethanol precipitation protocol by performing following steps.

a. The sequencing product was gently vortexed, shifted to 1.5 ml micro-centrifuge tube.

b. For 10 µl of the sequencing product, fresh stop solution was prepared by adding 2 µl Sodium Acetate including 1 µl of Glycogen and 2µl of Na-EDTA in another 1.5 ml micro-centrifuge tube.

c. In the sequencing product, 5 µl of stop solution and 65µl of chilled 100 % ethanol was added, gently vortexed and then centrifuged at 13,000 rpm for 20 minutes at 4°C.

d. The supernatant was discarded and the pellet was washed again with 150 µl of 70% chilled ethanol, centrifuged at 12,000 rpm for few minutes.

e. Washing step with 70% chilled ethanol was repeated.

f. Remove the supernatant and dried the pellet at 45°C in vacuum concentrator and then dissolved in 17 µl of Hi-Di formamide (HDF).

g. The purified products were then loaded onto a sample loading tray and processed for sequencing through Automated Genetic Analyzer, ABI Prism 310® (Applied Biosystem, USA).

Primer Designing

Primers were designed for coding exons of *GLI3*, and intron 5 of *LMBR1* (*ZRS/SHH*) using online available "Primer 3" software (http://frodo.mit.edu/primer3/). For checking the effect of variant in *ZRS* on *SHH*, Properties of amplified products were checked by UCSC and Ensemble genome browsers. The primer sequences are listed in table 2.7, and 2.8.

Analysis of Sequencing Data and Variant Validation

The sequencing data obtained after Sanger Sequencing was analyzed by using software Bio-Edit alignment editor version 7.1.3.0 (http://www.mbio.ncsu.edu/BioEdit/bioedit.html). Chromatogram of afflicted was evaluated with the corresponding reference (normal) gene sequence which was downloaded from Ensemble Genome Browser Database (http://www.ensembl.org/index.html) to find out any nucleotide change.

Additionally, if variation in affected sequence was documented, its pathogenicity was checked through MutationTaster(http://www.mutationtaster.org) or Polyphene-2 (http://genetics.bwh.harvard.edu/pph2/) software.

Table 2.6: Microsatellite Marker Used for Mapping Polydactyly

Sr.No	Gene	Location OR Cytogenetic band	Marker	cM
1	*GLI 1* Glioma-Associated Oncogene Homolog 1	12q13.3	D12S1724	70.52
			D12S1632	72.58
			D12S90	73.71
			D12S305	74.31
			D12S104	74.31
			D12S1298	74.31
			D12S1700	75.09
			D12S1056	75.09
			D12S1072	75.19
2	*GLI3* Glioma-Associated Oncogene Family Zinc Finger 3	7p13	D7S2541	60.90
			D7S2454	62.11
			D7S2548	62.57
			D7S691	62.99
			D7S2428	64.26
			D7S667	65.75
			D7S2427	66.58

3	*IQCE* IQ Domain-Containing Protein E	7p22.3	D7S2474	1.94
			D7S1532	3.12
			D7S616	4.79
			D7S2484	5.35
			D7S531	5.81
			D7S472	6.96
4	*ZNF141* Zinc Finger Protein 141	4p16.3	D4S90	0
			D4S2936	0.61
			D4S111	0.9
			D4S3038	0.9
			D4S43	2.86
5	*SHH/LMBR1* Sonic Hedgehog Protein/Limb Development Membrane Protein 1	7q36.3	D7S598	178.43
			D7S550	180.67
			D7S104	182.84
			D7S468	182.84
			D7S2423	185.38
			D7S54	186.09
6	*PITX1* Paired Like Home domain 1	5q31.1	D5S2057	136.27
			D5S2002	137.30
			D5S2117	138.54
			D5S2056	139.55
			D5S2115	140.06
			D5S816	141.18
			D5S479	142.23

7	*KIAA0825* Uncharacterized protein KIAA0825	5q15	D5S1725	103.13
			D5S815	105.5
			D5S2100	105.85
			D5S644	109.21
			D5S1462	109.58
			D5S1503	111.33
8	*FAM92A* Family with sequence similarity 92 member A1	8q22.1(8q21.13- q24.12)	D8S1697	98.57
			D8S1800	101.84
			GATA8B01	102.38
			D8S270	102.97
			D8S1818	103.15
			D8S1794	105.34
9	Chromosome 13	13q13.3-q21.2	D13S244	43.02
			D13S1227	44.74
			D13S887	47.47
			D13S1492	55.56
			D13S803	55.64
			D13S233	56.13
10	Locus at Chromosome 13	13q21-q32	D13S1306	73.25
			D13S1230	81
			D13S265	82.3
			D13S1300	83.19
			D13S627	89.29
			D13S1823	90.80

			D19S1034	18.21
11	Locus at Chromosome 19	19p13.1-13.2	D19S406	22.98
			D19S901	22.98
			D19S403	29.1
			D19S581	31.21
			D19S840	34.46
			D19S432	38.36
			D19S1171	40.3
			D19S915	44.26
			D19S566	45.27

Table 2.7: List of Primer Sequences to PCR-amplify *GLI 3*

Exon	Forward primer (Nucleotide Sequence5'-3')	Reverse primer(Nucleotide Sequence (5'-3')
1	CAGAAGGGATCGGATTACACGA	GGGTCGGACTCTTCGGAAA
2	GATACCAAACGCTCAGTAGGGA	GCAAACGCTCAATTCACAAGG
3	GAGGGATATCGAGAATGAGACC	AGACTGATGTTGCTTAGAGACG
4	TTTGAGTTGCAGTCAGTCCCA	ACCCACGAACAGATAGGCTTG
5	CACAAGGCTCCTTTGAATTCACTT	GTAAACCCCACTGCACGCTG
6	GGAATTGCTGATGTGGGTTGTGT	GGGGGTCTCAGGATGTCCAAA
7	TTGTCACCGCAAGTTGCCA	TCTTGGTATAGGCACAGCATCA
8	GCTTGGCAATAATCCTACCTTCT	ACACGTCCACCAAAACTGAAG
9	AAATAAGACCGCTTGTCCCG	ACTCCCAAGCTGCCTAAACT
10	ACTTCACAAAACCCTAGACCCA	CAATGCGGCTCCTAAGAAACT
11	GGTTAGGAAGCATGCATACAC	ACACCGAGGCATTTATCACC
12	CCATTGTCCACATTGAGCGG	AGTCCCACCTAGGAAGCTCA
13	GAACACCTCAAAGCCTTGTGAAA	TAAGCAATACGGGTCACTGCC
14	TGGTCCATCCGTCATTCTGG	TTAACGGATGGTTACAGCGTCA
15-a	GGGACACCAGAAATAGTTCCTAC	AGGCTCATCCTCTCCATGTTG
15-b	TACCGCCTCAAGGCCAAGTA	TCGTACCCTGCTTGGTTCTG
15-c	TCACCGAGAACGTCACCCT	CTCTTCAGCTTTGAGGCTTGAATC
15-d	TATGGGAACTGTCTCAACAGGC	CTTTCGTGTCTTGCTGACTGAAG
15-e	TGGTATCAAGATGGAGATGAAAGG	GTGAGATGAGATTGCTAAAATACATACAG

Table 2.8: List of Primers used for Sanger Sequencing *ZRS*

Sr.No	Forward Nucleotide sequence(5'-3')	Reverse Nucleotide sequence(5'-3')
ZRS-1	GCTGTGCTTATCATACCTCAGATT	GCACAATAGAGGAGGAACAAAGAT
ZRS-2	TGGAATGTCTATAAAGCTGAGCAA	TTGATTTTCCCAACACCTTCAAGA

Chapter 3

Results

Results

The present research study was conducted on four families (A, B, C, D) afflicted with polydactyly and originated from various regions of Pakistan, and Azad Jammu and Kashmir. Pedigrees, constructed with information provided by the elders, showed the disease phenotypes segregated in autosomal recessive form in three families. The fourth family showed autosomal dominant inheritance of the disease phenotype. The study was approved by Institutional Review Board (IRB) of Quaid-i-Azam University Islamabad.

Family A

This family was sampled from Rahimyar Khan district Sadiqabad province Punjab (Figure 1). Affected individuals of the family segregated non-syndromic polydactyly in an autosomal recessive form (Figure 3.2). Two afflicted (IV-1 and V-1) and normal members are (III-3, III-4, IV-2) participated in the present study. Blood samples from participated individuals were collected in EDTA-containing tubes.

Family B

Family B was sampled from a remote village of Azad Jammu and Kashmir (AJK) near at India-Pakistan border. This is a five generation pedigree having four affected individuals. Three normal persons (IV-1, IV-2, and V-4) and two afflicted persons (IV-3, V-1) participated in the study (Figure 3.3). Clinical pictures of affected individuals depicted that the family segregated non-syndromic preaxial polydactyly (PPD) in autosomal recessive form (Figure 3.4). Blood samples from two afflicted and three normal members were taken in EDTA tubes for DNA extraction.

Family C

Family C was located in Azad Jammu and Kashmir (AJK),an independent state of Pakistan. Family pedigree showed an autosomal recessive inheritance of the disease (Figure 3.5). Examination of autopods of affected individuals showed post-axial polydactyly in two while preaxial polydactyly in the third affected individual. The

disease phenotypes were present only in upper limbs. Lower limbs of the affected individuals presented normal anatomy. All the affected individuals had normal intellectual and hearing abilities, with normal height and weight. Blood samples from three affected (II-4, II-5, III-3) and three normal individuals (I-1, 1-2, III-3) were collected for DNA extraction.

Family D

Family D, recruited for this study, was the permanent resident of Rawalpindi, Punjab province of the country. The disease phenotypes segregated in three consecutive generations of the pedigree with at least one affected in each generation, thus proving the dominant inheritance of the disease (Figure 3.7). Clinical examination of the affected individuals showed features of non-syndromic bilateral postaxial Polysyndactyly (Figure 3.8).

Homozygosity Mapping and Sanger Sequencing

A well-known technique of homozygosity mapping based on typing microsatellite markers and Sanger sequencing were used to solve three families(A, B, C), inheriting the disorders in autosomal recessive manner at genetic level. Detailed protocols used for homozygosity mapping and Sanger sequencing are described in chapter 2 Materials and Methods. Linkage in the three families was tested to eight candidate genes including *GLI1* (12q13.3), *ZNF141* (4p16.3), *IQCE* (7p22.3), *FAM92A* (8q22.1), *PITX1* (5q31.1), *GLI3* (7p13), *SHH* (7q36.3), and *KIAA0825* (5q15). In addition, markers mapped at chromosome13q13.3-q21.2 and 13q21-q32 was typed as well (Table 2.6). All markers genotyped showed heterozygous pattern of alleles in both affected and unaffected individuals of three families (A, B, C). Thus no homozygous region was found shared by all affected individuals in a respective family at any locus tested for genotyping. Therefore, linkage in the three families to tested genes was considered as excluded.

The fourth family (D) showed autosomal dominant inheritance of the disease. Three previously reported genes including *GLI3*, *SHH*, and intron 5 of *LMBR1(ZRS/SHH)*, involved in causing polydactyly, were sequenced in affected and unaffected members of the family. Sequence analysis revealed a novel variation (g.101537T>C; c.1034 +

182 T>C) in intron 5 of the *LMBR1*. Freely available online mutation effect prediction tool MutationTaster predicted the identified variant as disease causing. The frequency of the variant was zero in gnomAD and Human Genome Mutation Database.
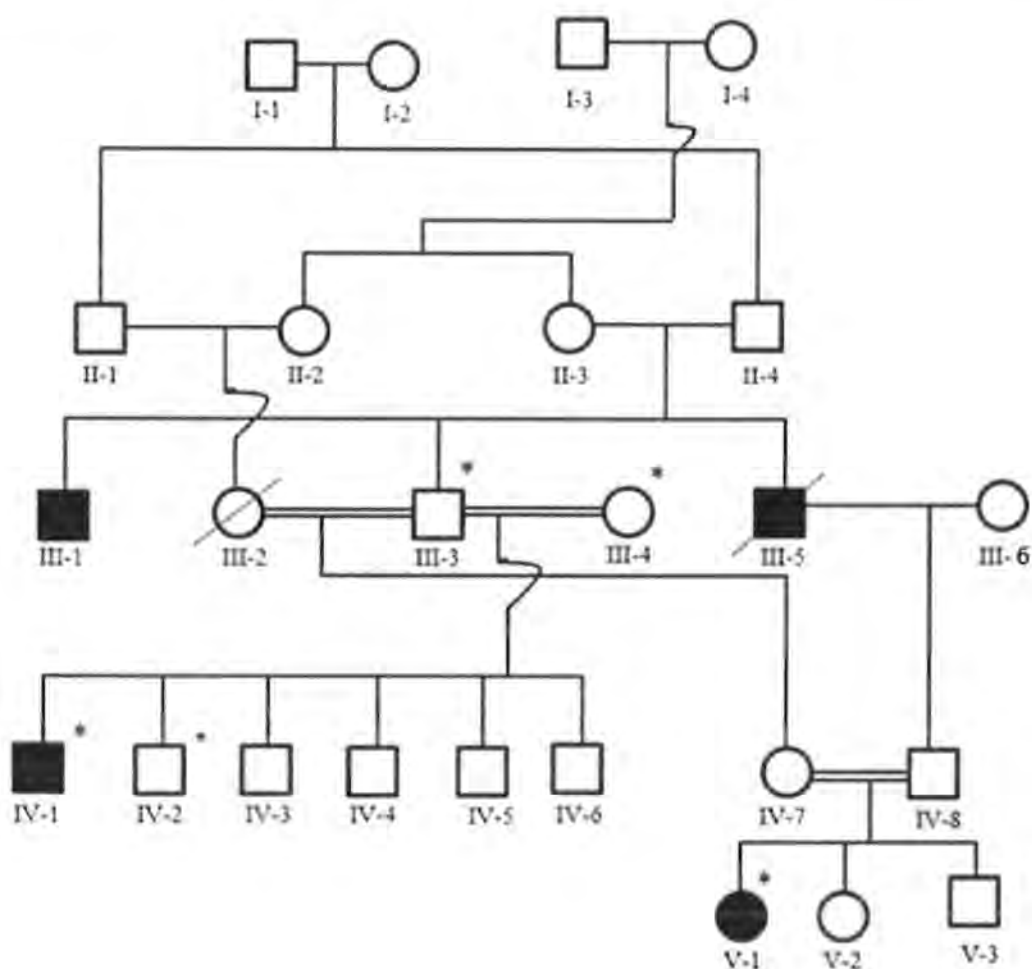
Figure 3.1: Pedigree of the family A with hereditary preaxial polydactyly. Symbols of Squares and circles represent male and females, respectively. Unfilled symbols are used for normal individuals while filled represent affected members. Consanguineous marriages are indicated by double lines. Slashed lines depict the departed individuals. Roman numerals are used for indicating generation number while Arabic numbers indicating the number of individuals in the pedigree. Asterisk (*) labeled shapes are symbolizing the individuals whose blood samples were available to carry out the study.
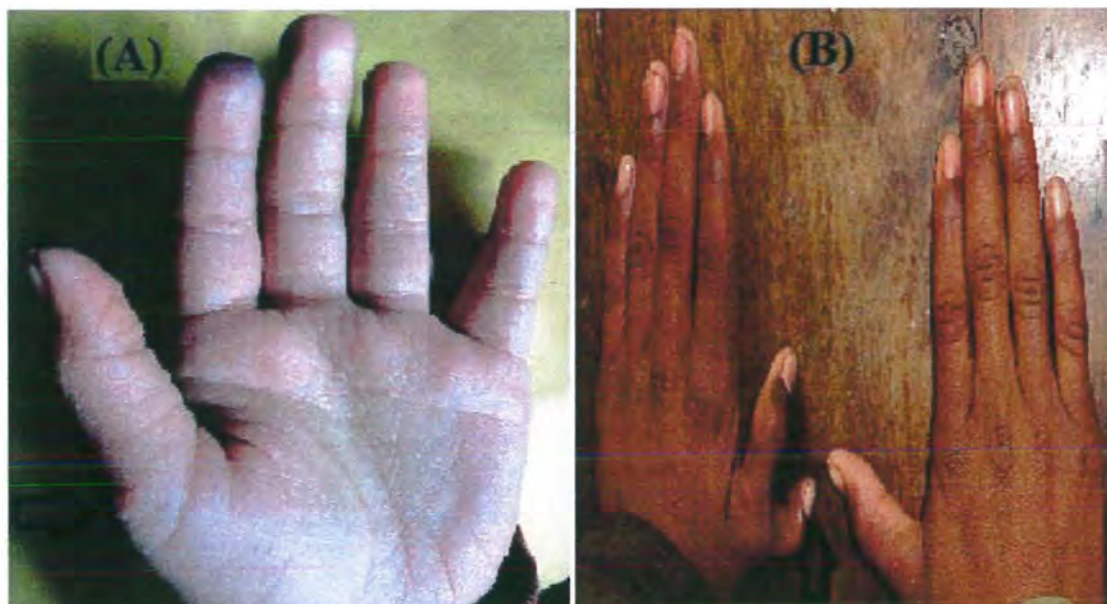
Figure 3.2: Affected member (V-1) of family A showing preaxial polydactyly which was surgically removed at time of birth. A small skin tag remained after surgical removal of the extra digit is shown with an arrow (A).Patient (VI-1) depicting the presence of fully developed finger at the radial side of left hand (preaxial polydactyly).
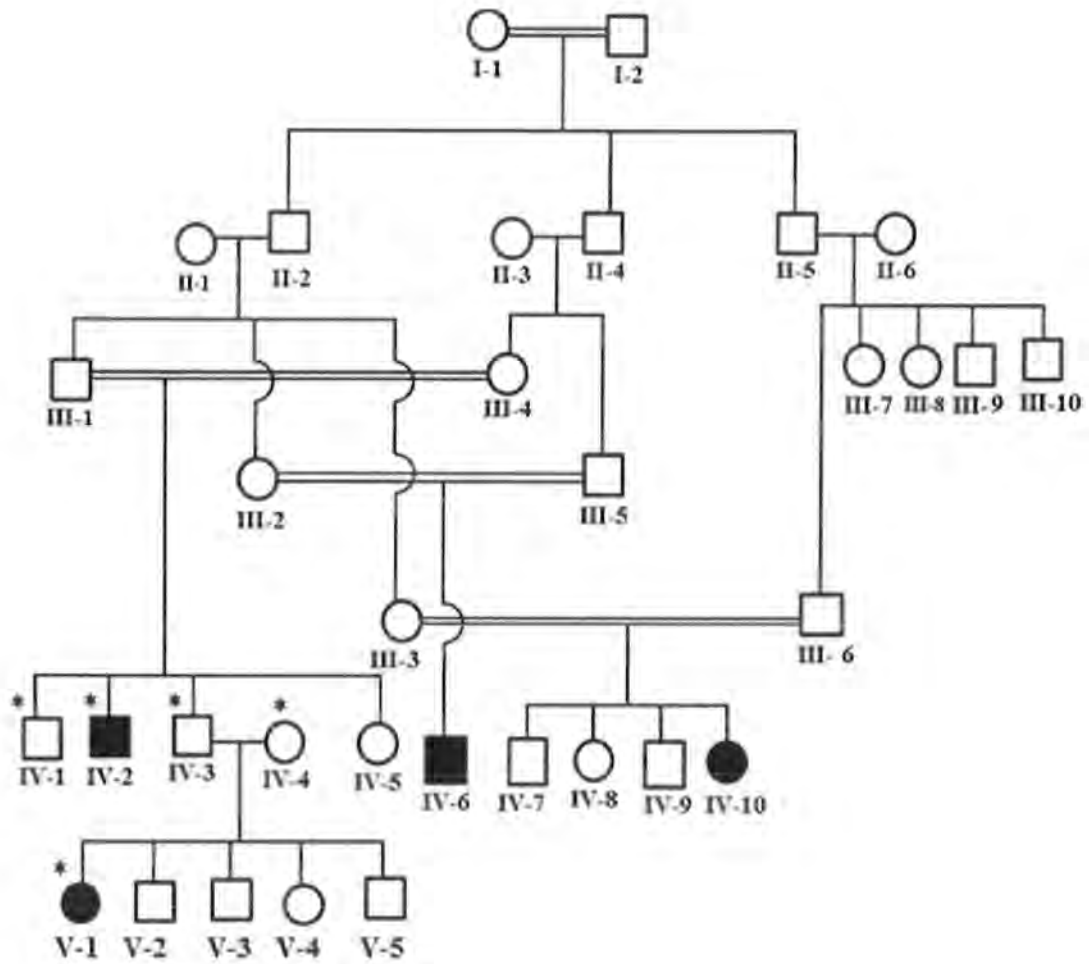
Figure 3.3: Pedigree of the family B with hereditary preaxial polydactyly. Squares and circles represent male and females, respectively. Unfilled symbols are used for normal individuals while filled represent affected members of the family. Consanguineous marriages are indicated by double lines. Roman numerals are used for indicating generation number while Arabic numbers indicating the number of individuals in the pedigree. Asterisk (*) labeled shapes are symbolizing the individuals whose blood samples were available to carry out the study.

Figure 3.4 Clinical features of affected individuals in family B. Affected member (IV- 2) showing an extra non-functional digit cutaneously fused with great thumb in left hand (A).Patient (V-1) showing extra digit with fully developed nail pointed towards thumb in right hand.
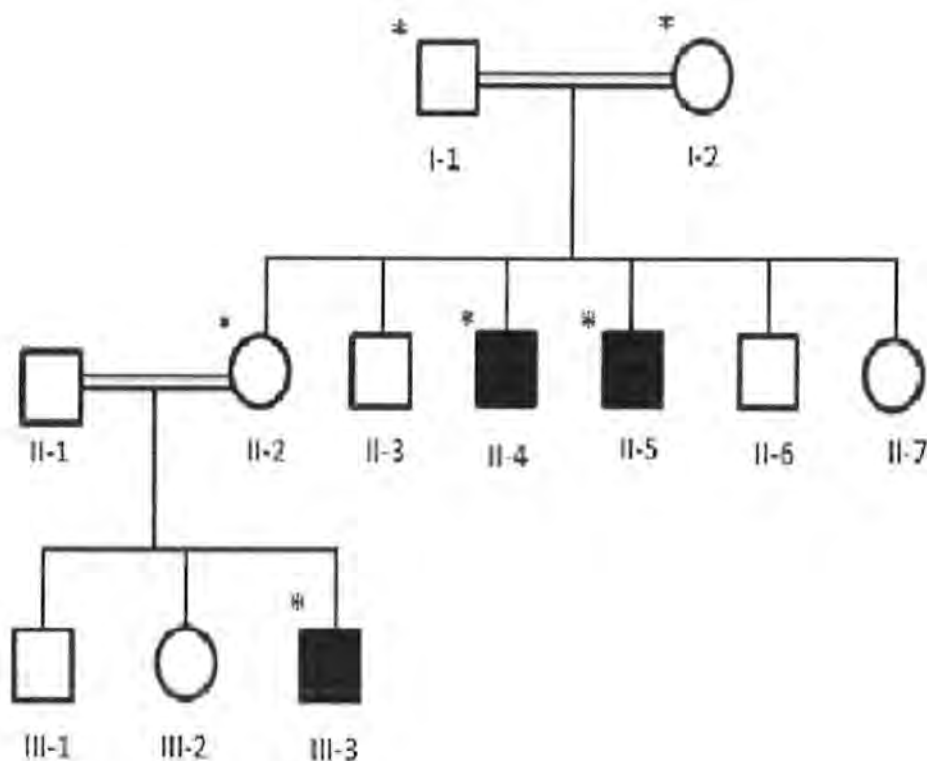
Figure 3.5: Pedigree of the family C with hereditary postaxial and preaxial polydactyly. Squares and circles represent male and females, respectively. Unfilled symbols are used for normal individuals while filled affected members. Consanguineous marriages are indicated by double lines. Roman numerals are used for indicating generation number while Arabic numbers indicating the number of individuals in the pedigree. Asterisk (*) labeled shapes are symbolizing the individuals whose blood samples were available to carry out the study.
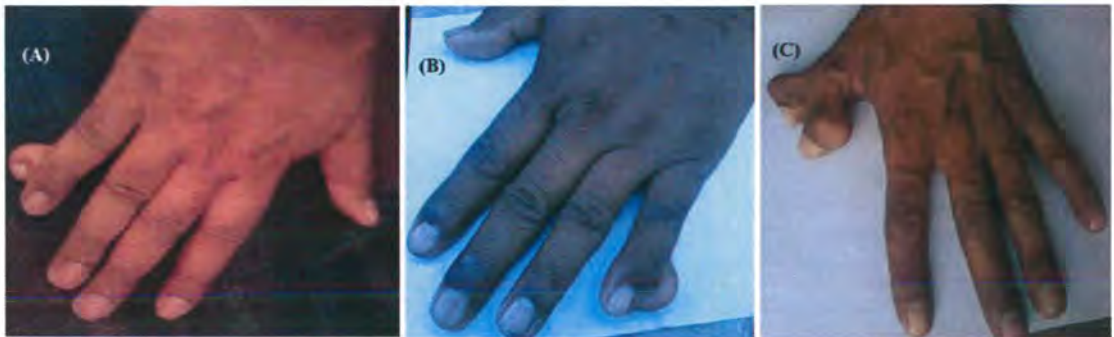
Figure 3.6: Clinical features of affected individuals of family C. Patient (II-4) showing postaxial polydactyly in right hand (A). Patient (II-5) is showing postaxial polydactyly in left hand (B). Affected member (III-3) showing duplicated thumb, turning towards palm at proximal-distal phalangeal joint illustrating preaxial polydactyly (C).
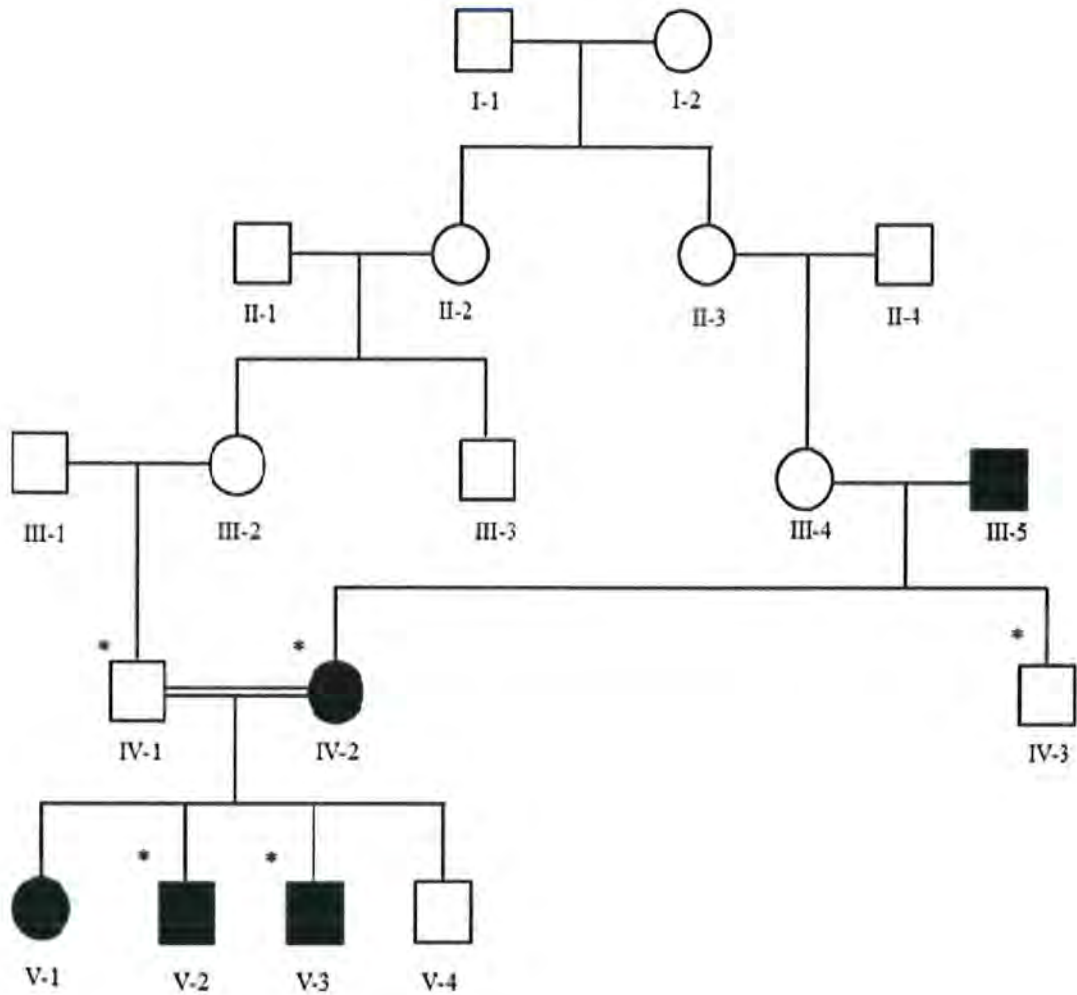
Figure 3.7: Pedigree of the family B with hereditary postaxial polydactyly. Squares and circles represent male and females, respectively. Unfilled symbols are used for normal individuals while filled affected members of the family. Consanguineous marriages are indicated by double lines. Roman numerals are used for indicating generation number while Arabic numbers indicating the number of individuals in the pedigree. Asterisk (*) labeled shapes are symbolizing the individuals whose blood samples were available to carry out the study.

Figure 3.8: Clinical features of affected individuals of family D. Feet of affected individual (IV-2) showing bilateral postaxial polydactyly (A).Hands of patient (V-3) showing bilateral postaxial polydactyly and unilateral syndactyly of digits 4-5 in right hand (B).

Microsatellite results

FamilyA→*GLI1*

STS	cM	Normal III-3	Normal III-4	Normal IV-2	Affected IV-1	Affected V-1
D12S1724	70.52					
D12S1632	72.58					
D12S305	74.31					
D12S104	74.31					
D12S1700	75.09					
D12S1056	75.09					
D12S1072	75.19					

Figure 3.9 Allelic arrangements obtained with microsatellite markers linked to candidate gene *GLI1* in ethidium bromide stained Electropherograms. The Roman with Arabic numerals indicate family members of the pedigree.

Family A →*GLI3*

STS	cM	Normal III-3	Normal III-4	Normal IV-2	Affected IV-1	Affected V-1
D7S2454	62.11					
D7S2548	62.57					
D7S691	62.99					
D7S2428	64.26					
D7S667	65.75					
D7S2427	66.58					

Figure 3.10: Allelic arrangements obtained with microsatellite markers linked to candidate gene *GLI3* in ethidium bromide stained Electropherograms. The Roman with Arabic numerals indicates family members of the pedigree.

Family A → *IQCE*
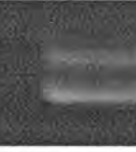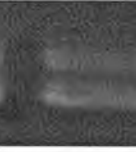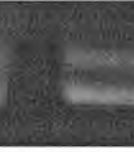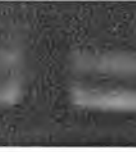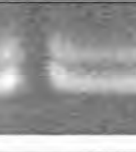
STS	cM	Normal III-3	Normal III-4	Normal IV-2	Affected IV-1	Affected V-1
D7S2474	1.94					
D7S1532	3.12					
D7S616	4.79					
D7S2484	5.35					
D7S531	5.81					
D7S472	6.96					

Figure 3.11: Allelic arrangements obtained with microsatellite markers linked to candidate gene *IQCE* in ethidium bromide stained Electropherograms. The Roman with Arabic numerals indicates family members of the pedigree.

Family A→*ZNF141*
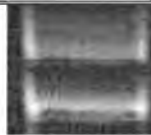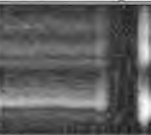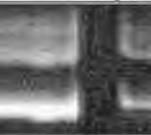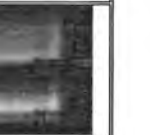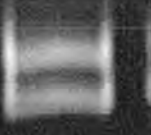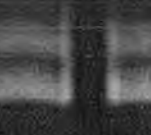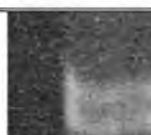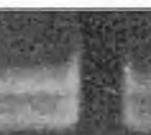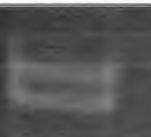
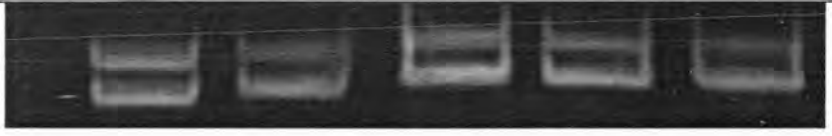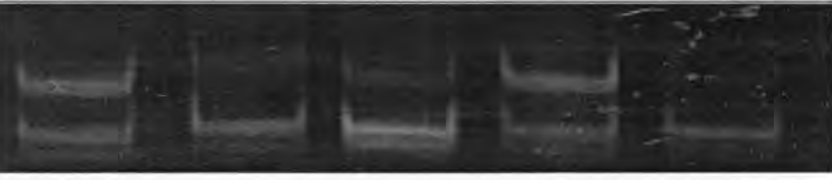| STS	cM	Normal III-3	Normal III-4	Normal IV-2	Affected IV-1	Affected V-1
D4S90	0					
D4S2936	0.61					
D4S111	0.9					
D4S3038	0.9					
D4S43	2.86					
D4S412	3.6					

Figure 3.12: Allelic arrangements obtained with microsatellite markers linked to candidate gene *ZNF141* in ethidium bromide stained Electropherograms. The Roman with Arabic numerals indicate family members of the pedigree.
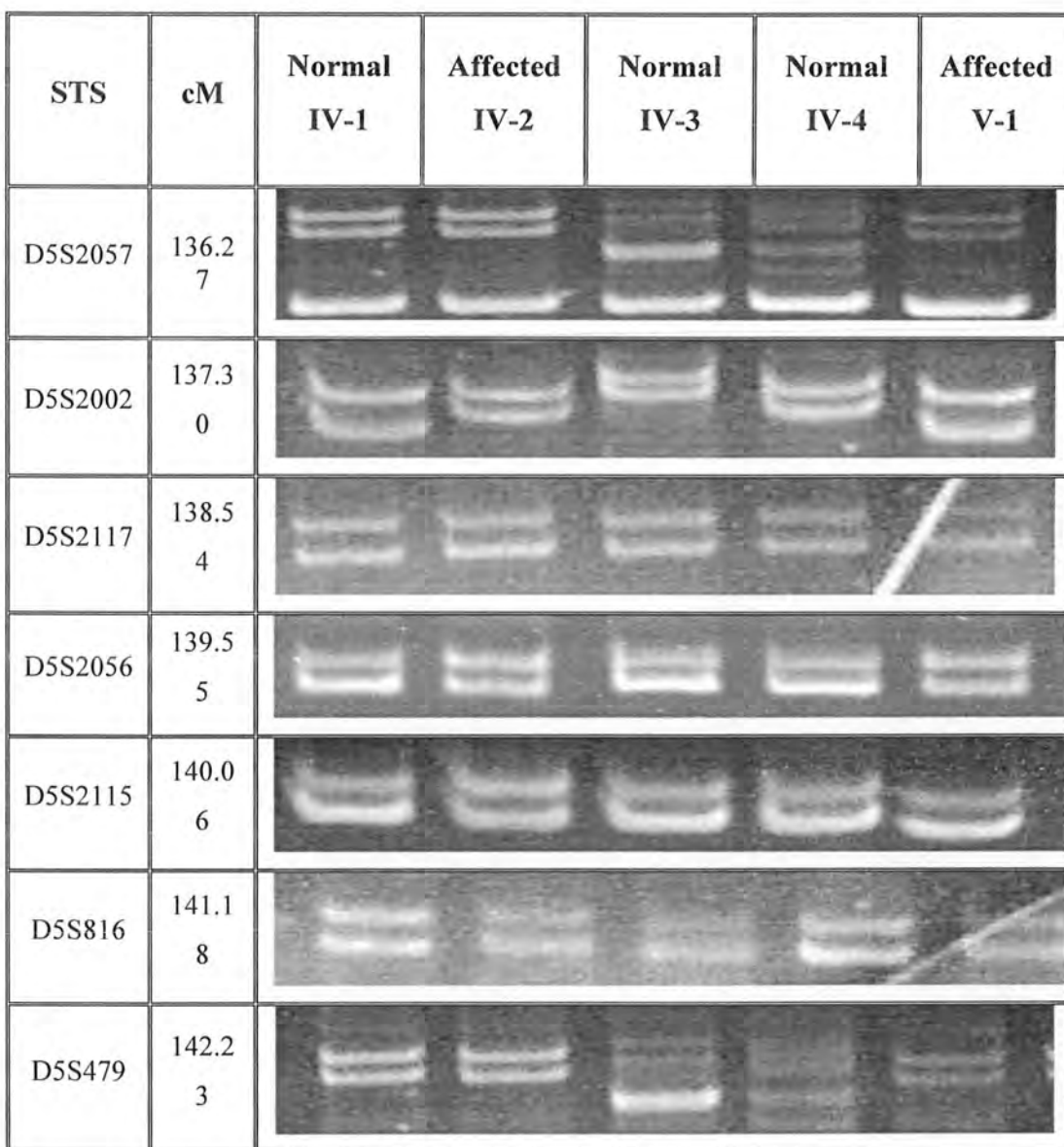
Family A →*SHH/LMBR1*
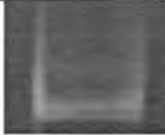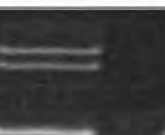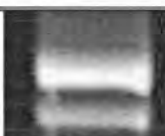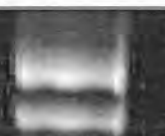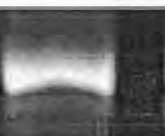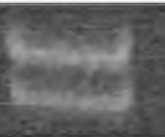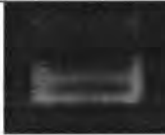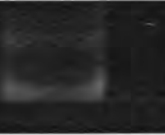
STS	cM	Normal III-3	Normal III-4	Normal IV-2	Affected IV-1	Affected V-1
D7S598	178.43					
D7S550	180.67					
D7S104	182.84					
D7S468	182.84					
D7S2423	185.38					
D7S54	186.09					

Figure 3.13: Allelic arrangements obtained with microsatellite markers linked to candidate gene *SHH/LMBR1* in ethidium bromide stained Electropherograms. The Roman with Arabic numerals indicate family members of the pedigree.

Family A→*PITXI* (5q31.1)

STS	cM	Normal III-3	Normal III-4	Normal IV-2	Affected IV-1	Affected V-1
D5S2057	136.27					
D5S2002	137.30					
D5S2117	138.54					
D5S2056	139.55					
D5S2115	140.06					
D5S816	141.18					

Figure 3.14: Allelic arrangements obtained with microsatellite markers linked to candidate gene*PITXI* in ethidium bromide stained Electropherograms. The Roman with Arabic numerals indicates family members of the pedigree.

Family A→*KIAA0825* **(5q15)**

STS	cM	Normal III-3	Normal III-4	Normal IV-2	Affected IV-1	Affected V-1
D5S1725	103.13					
D5S815	105.5					
D5S2100	105.85					
D5S644	109.21					
D5S1462	109.58					
D5S1503	111.33					
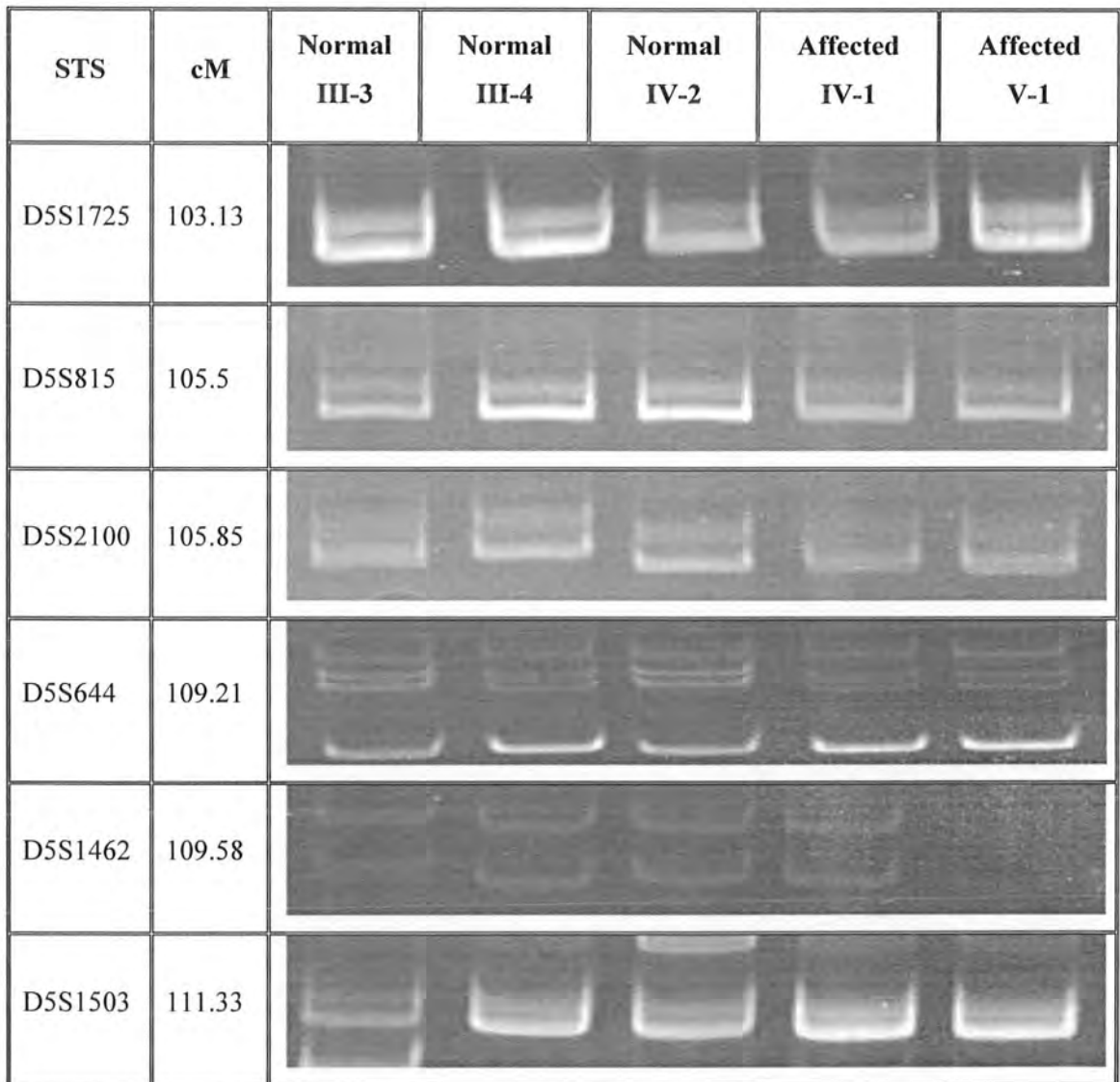
Figure 3.15: Allelic arrangements obtained with microsatellite markers linked to candidate gene *KIAA0825* in ethidium bromide stained Electropherograms. The Roman with Arabic numerals indicates family members of the pedigree.

Family A →*FAM92A* (8q21.13-q24.12)

STS	cM	Normal III-3	Normal III-4	Normal IV-2	Affected IV-1	Affected V-1
D8S1697	98.57					
D8S1800	101.84					
GATA8BO 1	102.38					
D8S270	102.97					
D8S1818	103.15					
D8S1794	105.34					

Figure 3.16: Allelic arrangements obtained with microsatellite markers linked to candidate gene *FAM92A* in ethidium bromide stained Electropherograms. The Roman with Arabic numerals indicate family members of the pedigree.

Family A→Chromosome 13 (locus 13q13.3-q21.2)
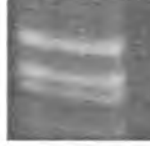
STS	cM	Normal III-3	Normal III-4	Normal IV-2	Affected IV-1	Affected V-1
D13S244	43.02					
D13S1227	44.74					
D13S887	47.47					
D13S1492	55.56					
D13S803	55.64					
D13S233	56.13					

Figure 3.17: Allelic arrangements obtained with microsatellite markers linked to candidate locus 13q13.3-q21.2 (Chromosome 13)in ethidium bromide stained Electropherograms. The Roman with Arabic numerals indicate family members of the pedigree.

Family A →Chromosome 13 (Locus 13 13q21-q32)

STS	cM	Normal III-3	Normal III-4	Normal IV-2	Affected IV-1	Affected V-1
D13S1306	81					
D13S1230	82.3					
D13S265	83.19					
D13S1300	89.29					
D13S627	90.12					
D13S1823	90.80					

Figure 3.18: Allelic arrangements obtained with microsatellite markers linked to candidate Locus 13 13q21-q32 (Chromosome 13) in ethidium bromide stained Electropherograms. The Roman with Arabic numerals indicate family members of the pedigree
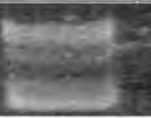
Family A →CHROMSOME 19(locus 19p13.1-13)

STS	cM	Normal III-3	Normal III-4	Normal IV-2	Affected IV-1	Affected V-1
D19S901	22.98					
D19S403	29.1					
D19S581	31.21					
D19S840	34.46					
D19S432	38.36					
D19S1171	40.3					
D19S915	44.26					

Figure 3.19: Allelic arrangements obtained with microsatellite markers linked to candidate Locus 19p13.1-13 (Chromosome 19) in ethidium bromide stained Elect ropherograms. The Roman with Arabic numerals indicate family members of the pedigree

Microsatellite results

Family B → *GLI 1*
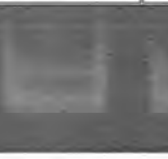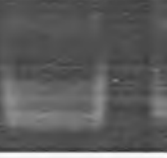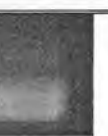
STS	cM	Normal IV-1	Affected IV-2	Normal IV-3	Normal IV-4	Affected V-1
D12S1632	72.58					
D12S90	73.71					
D12S305	74.31					
D12S104	74.31					
D12S1700	75.09					
D12S1072	75.19					

Figure 3.20: Allelic arrangements obtained with microsatellite markers linked to candidate gene *GLI1* in ethidium bromide stained Electropherograms. The Roman with Arabic numerals indicate family members of the pedigree

Family B → *GLI 3*

STS	cM	Normal IV-1	Affected IV-2	Normal IV-3	Normal IV-4	Affected V-1
D7S2541	60.90					
D7S2454	62.11					
D7S691	62.99					
D7S2428	64.26					
D7S667	65.75					
D7S2427	66.58					

Figure 3.21: Allelic arrangements obtained with microsatellite markers linked to candidate gene *GLI3* in ethidium bromide stained Electropherograms. The Roman with Arabic numerals indicate family members of the pedigree

Family B →*IQCE*
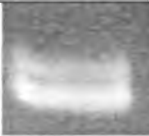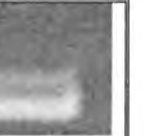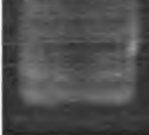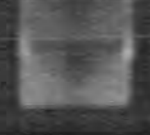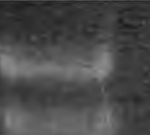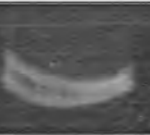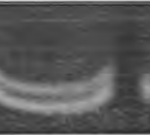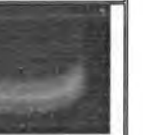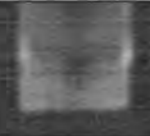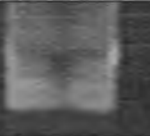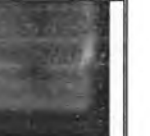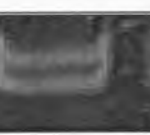
STS	cM	Normal IV-1	Affected IV-2	Normal IV-3	Normal IV-4	Affected V-1
D7S2474	1.94					
D7S1532	3.12					
D7S616	4.79					
D7S2484	5.35					
D7S531	5.81					
D7S472	6.96					

Figure 3.22: Allelic arrangements obtained with microsatellite markers linked to candidate gene *IQCE* in ethidium bromide stained Electropherograms. The Roman with Arabic numerals indicate family members of the pedigree

Family B →*ZNF141*

STS	cM	Normal IV-1	Affected IV-2	Normal IV-3	Normal IV-4	Affected V-1
D4S90	0					
D4S2936	0.61					
D4S111	0.9					
D4S3038	0.9					
D4S43	2.86					
D4S412	3.6					
D4S2957	5.72					

Figure 3.23: Allelic arrangements obtained with microsatellite markers linked to candidate gene *ZNF141* in ethidium bromide stained Electropherograms. The Roman with Arabic numerals indicate family members of the pedigree

Family B → *SHH/LMBR1*
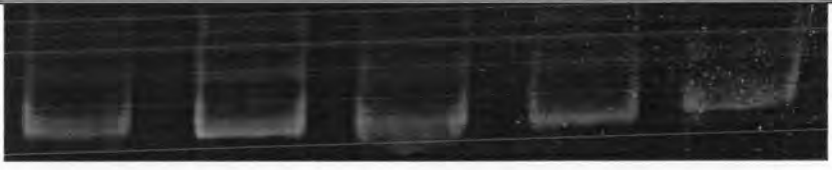
STS	cM	Normal IV-1	Affected IV-2	Normal IV-3	Normal IV-4	Affected V-1
D7S598	178.43					
D7S550	180.67					
D7S104	182.84					
D7S468	182.84					
D7S2423	185.38					
D7S54	186.09					

Figure 3.24: Allelic arrangements obtained with microsatellite markers linked to candidate gene *SHH/LMBR1* in ethidium bromide stained Electropherograms. The Roman with Arabic numerals indicate family members of the pedigree
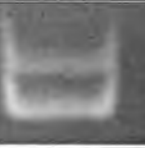
Family B →*PITXI* (5q31.1)

STS	cM	Normal IV-1	Affected IV-2	Normal IV-3	Normal IV-4	Affected V-1
D5S2057	136.2 7					
D5S2002	137.3 0					
D5S2117	138.5 4					
D5S2056	139.5 5					
D5S2115	140.0 6					
D5S816	141.1 8					
D5S479	142.2 3					

Figure 3.25: Allelic arrangements obtained with microsatellite markers linked to candidate gene *PITXI* in ethidium bromide stained Electropherograms. The Roman with Arabic numerals indicate family members of the pedigree

Family B→*KIAA0825* (5q15)
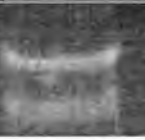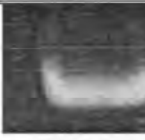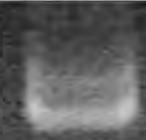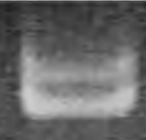
STS	cM	Normal IV-1	Affected IV-2	Normal IV-3	Normal IV-4	Affected V-1
D5S1725	103.13					
D5S815	105.5					
D5S2100	105.85					
D5S644	109.21					
D5S1462	109.58					
D5S1503	111.33					

Figure 3.26: Allelic arrangements obtained with microsatellite markers linked to candidate gene *KIAA0825* in ethidium bromide stained Electropherograms. The Roman with Arabic numerals indicate family members of the pedigree

Family B→*FAM92A* (8q21.13-q24.12)
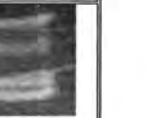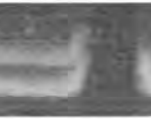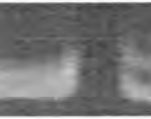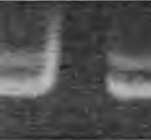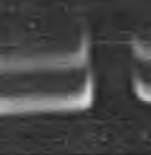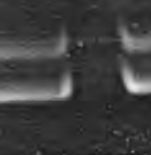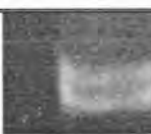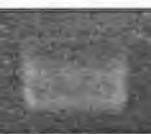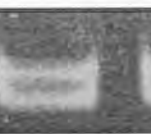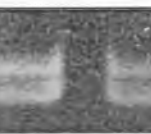
STS	cM	Normal IV-1	Affected IV-2	Normal IV-3	Normal IV-4	Affected V-1
D8S1697	98.57					
D8S1800	101.8 4					
GATA8BO 1	102.3 8					
D8S270	102.9 7					
D8S1818	103.1 5					
D8S1794	105.3 4					

Figure 3.27: Allelic arrangements obtained with microsatellite markers linked to candidate gene *FAM92A* in ethidium bromide stained Electropherograms. The Roman with Arabic numerals indicate family members of the pedigree

Family B →CHROMOSOME 13 (locus 13q13.3-q21.2)
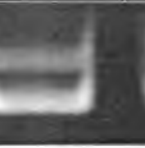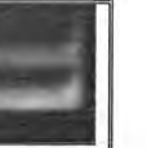
STS	cM	Normal IV-1	Affected IV-2	Normal IV-3	Normal IV-4	Affected V-1
D13S244	43.02					
D13S1227	44.74					
D13S887	47.47					
D13S1492	55.56					
D13S803	55.64					
D13S233	56.13					

Figure 3.28: Allelic arrangements obtained with microsatellite markers linked to candidate locus 13q13.3-q21.2 (Chromosome 13) in ethidium bromide stained Electropherograms. The Roman with Arabic numerals indicate family members of the pedigree

Family B→   Chromosome 13 (Locus 13q21-q32)

STS	cM	Normal IV-1	Affected IV-2	Normal IV-3	Normal IV-4	Affected V-1
D13S1306	73.25					
D13S1230	81					
D13S265	82.3					
D13S1300	83.19					
D13S627	89.29					
D13S1280	90.12					
D13S1823	90.80					

Figure 3.29: Allelic arrangements obtained with microsatellite markers linked to candidate Locus 13q21-q32 (Chromosome 13) in ethidium bromide stained Electropherograms. The Roman with Arabic numerals indicate family members of the pedigree

Family B→CHROMSOME 19 (locus 19p13.1-13.2)

STS	cM	Normal IV-1	Affected IV-2	Normal IV-3	Normal IV-4	Affected V-1
D19S1034	18.21					
D19S901	22.98					
D19S403	29.1					
D19S581	31.21					
D19S840	34.46					
D19S432	38.36					
D19S1171	40.3					

Figure 3.30: Allelic arrangements obtained with microsatellite markers linked to candidate Locus 19p13.1-13.2 (Chromosome 19) in ethidium bromide stained Electropherograms. The Roman with Arabic numerals indicate family members of the pedigree.

Microsatellite results

Family C →*GLI1*

STS	cM	Normal I-1	Normal I-2	Normal I-3	Affected II-4	Affected II-5	Affected III-3
D12S1724	70.52						
D12S90	73.71						
D12S305	74.31						
D12S104	74.31						
D12S1700	75.09						
D12S1072	75.19						

Figure 3.31: Allelic arrangements obtained with microsatellite markers linked to candidate gene *GLI1* in ethidium bromide stained Electropherograms. The Roman with Arabic numerals indicate family members of the pedigree.

Family C→*GLI 3*
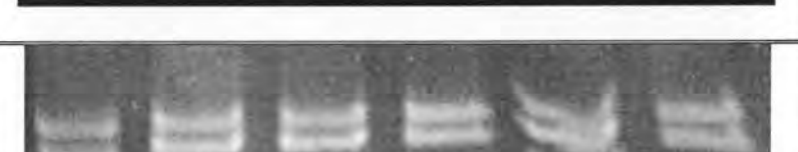
STS	cM	Normal I-1	Normal I-2	Normal I-3	Affected II-4	Affected II-5	Affected III-3
D7S2541	60.90						
D7S2454	62.11						
D7S2548	62.57						
D7S691	62.99						
D7S2428	64.26						
D7S667	65.75						
D7S2427	66.58						

Figure 3.32: Allelic arrangements obtained with microsatellite markers linked to candidate gene *GLI3* in ethidium bromide stained Electropherograms. The Roman with Arabic numerals indicate family members of the pedigree.

Family C →*IQCE*
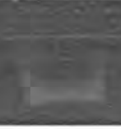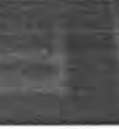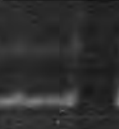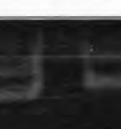
STS	cM	Normal I-1	Normal I-2	Normal I-3	Affected II-4	Affected II-5	Affected III-3
D7S2474	1.94						
D7S1532	3.12						
D7S616	4.79						
D7S2484	5.35						
D7S531	5.81						
D7S472	6.96						

Figure 3.33: Allelic arrangements obtained with microsatellite markers linked to candidate gene *IQCE* in ethidium bromide stained Electropherograms. The Roman with Arabic numerals indicate family members of the pedigree

Family C→*ZNF141*
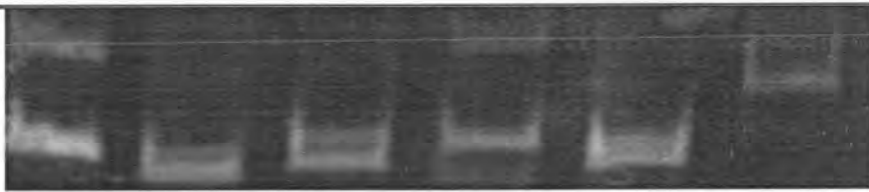
STS	cM	Normal I-1	Normal I-2	Normal I-3	Affected II-4	Affected II-5	Affected III-3
D4S90	0						
D4S3360	0						
D4S2936	0.61						
D4S111	0.9						
D4S412	3.6						
D4S2957	5.72						

Figure 3.34: Allelic arrangements obtained with microsatellite markers linked to candidate gene *ZNF141* in ethidium bromide stained Electropherograms. The Roman with Arabic numerals indicate family members of the pedigree
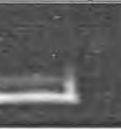
Family C→*SHH/LMBR1*

STS	cM	Normal I-1	Normal I-2	Normal I-3	Affected II-4	Affected II-5	Affected III-3
D7S598	178.43						
D7S550	180.67						
D7S104	182.84						
D7S468	182.84						
D7S2423	185.38						
D7S54	186.09						

Figure 3.35: Allelic arrangements obtained with microsatellite markers linked to candidate gene *SHH/LMBR1* in ethidium bromide stained Electropherograms. The Roman with Arabic numerals indicate family members of the pedigree

Family C →*PITX1* (5q31.1)

STS	cM	Normal I-1	Normal I-2	Normal I-3	Affected II-4	Affected II-5	Affected III-3
D5S2057	136.27						
D5S2002	137.30						
D5S2117	138.54						
D5S2056	139.55						
D5S2115	140.06						
D5S816	141.18						
D5S479	143.23						

Figure 3.36: Allelic arrangements obtained with microsatellite markers linked to candidate gene *PITX1* in ethidium bromide stained Electropherograms. The Roman with Arabic numerals indicate family members of the pedigree

Family C →*KIAA0825*
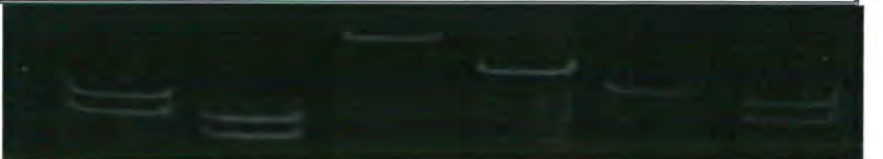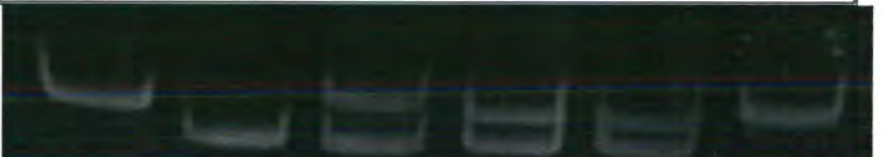
STS	cM	Normal I-1	Normal I-2	Normal I-3	Affected II-4	Affected II-5	Affected III-3
D5S1725	103.13						
D5S815	105.5						
D5S2100	105.85						
D5S644	109.21						
D5S1462	109.58						
D5S1503	111.33						

Figure 3.37: Allelic arrangements obtained with microsatellite markers linked to candidate gene *KIAA0825* in ethidium bromide stained Electropherograms. The Roman with Arabic numerals indicate family members of the pedigree.

Family C→*FAM92A* (8q21.13-q24.12)
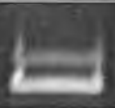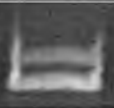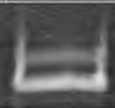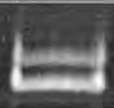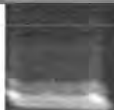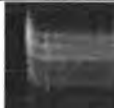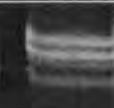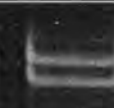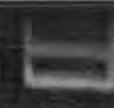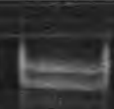
STS	cM	Normal I-1	Normal I-2	Normal I-3	Affected II-4	Affected II-5	Affected III-3
D8S1697	98.57						
D8S1800	101.84						
GATA8BO1	102.38						
D8S270	102.97						
D8S1818	103.15						
D8S1794	105.34						

Figure 3.38: Allelic arrangements obtained with microsatellite markers linked to candidate gene *FAM92A* in ethidium bromide stained Electropherograms. The Roman with Arabic numerals indicate family members of the pedigree

Family C→CHROMOSOME 13 (13q13.3-q21.2)
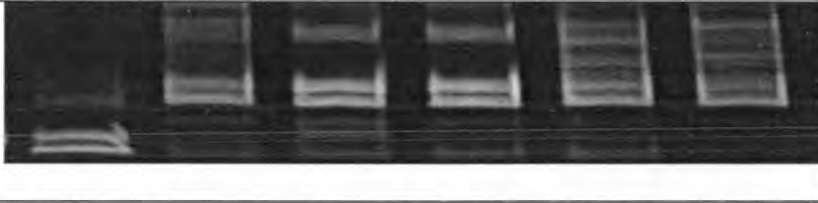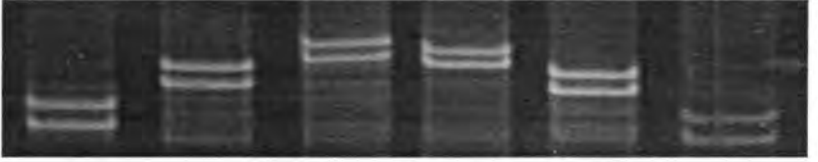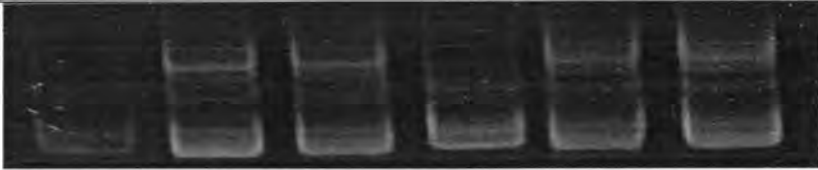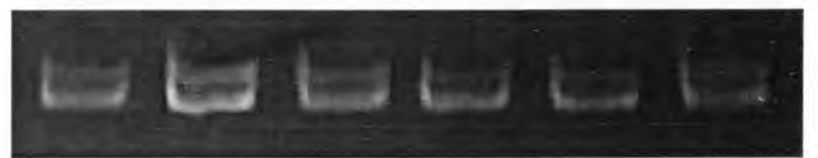
STS	cM	Normal I-1	Normal I-2	Normal I-3	Affected II-4	Affected II-5	Affected III-3
D13S244	43.02						
D13S122 7	44.74						
D13S887	47.47						
D13S149 2	55.56						
D13S803	55.64						
D13S233	56.13						

Figure 3.39: Allelic arrangements obtained with microsatellite markers linked to candidate Locus 13q13.3-q21.2 (Chromosome 13) in ethidium bromide stained Electropherograms. The Roman with Arabic numerals indicate family members of the pedigree

Family C →Chromosome 13 13q21-q32
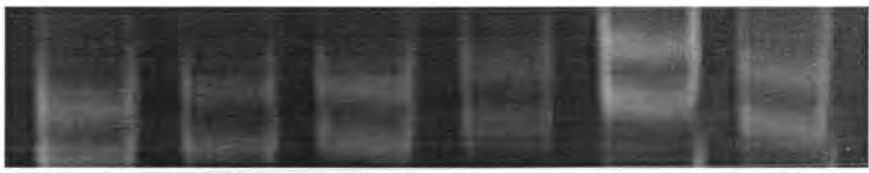
STS	cM	Normal I-1	Normal I-2	Normal I-3	Affected II-4	Affected II-5	Affected III-3
D13S1306	73.25						
D13S1306	81						
D13S1230	82.3						
D13S265	83.19						
D13S1300	89.29						
D13S627	90.12						
D13S1823	90.80						

Figure 3.40: Allelic arrangements obtained with microsatellite markers linked to candidate. Locus13q21-q32 (Chromosome13) in ethidium bromide stained Electropherograms. The Roman with Arabic numerals indicate family members of the pedigree

Family C →CHROMOSOME # 19*(locus 19p13.1-13.2)*
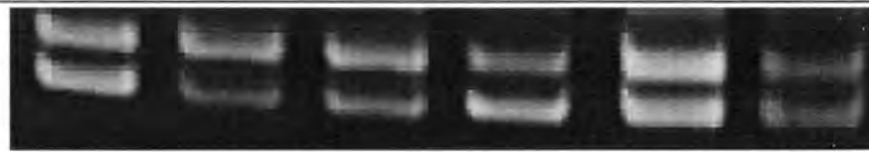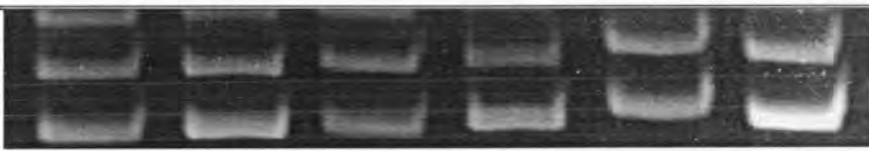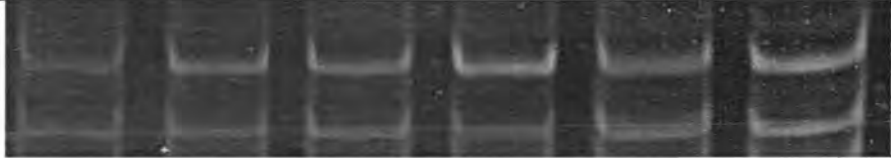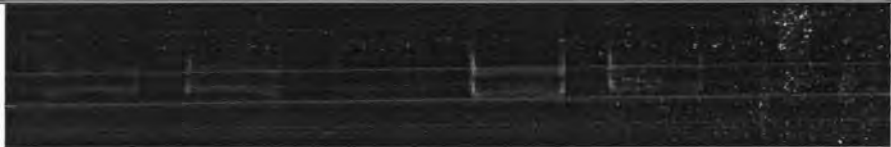
STS	cM	Normal I-1	Normal I-2	Normal I-3	Affected II-4	Affected II-5	Affected III-3
D19S90 1	22.9 8						
D19S40 3	29.1						
D19S58 1	31.2 1						
D19S84 0	34.4 6						
D19S43 2	38.3 6						
D19S56 6	45.2 7						

Figure 3.41: Allelic arrangements obtained with microsatellite markers linked to candidate *locus* 19p13.1-13.2(Chromosome 19)inethidium bromide stained Electropherograms. The Roman with Arabic numerals indicate family members of the pedigree
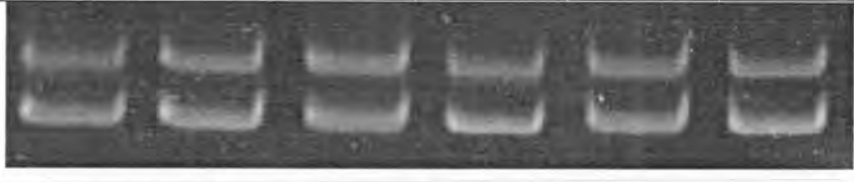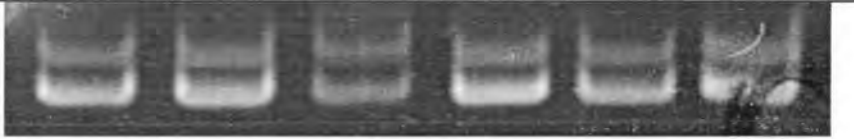
(A) Heterozygous Affected   c.423+4695 T>C

C T G A T A A T A A A A G C A A A A A G N A C A A A A T T T T A G G T A A C T T C

(B) Wild Type Normal   c.423+4695 T>T

C T G A T A A T A A A A G C A A A A A G T A C A A A A T T T T A G G T A A C T T C
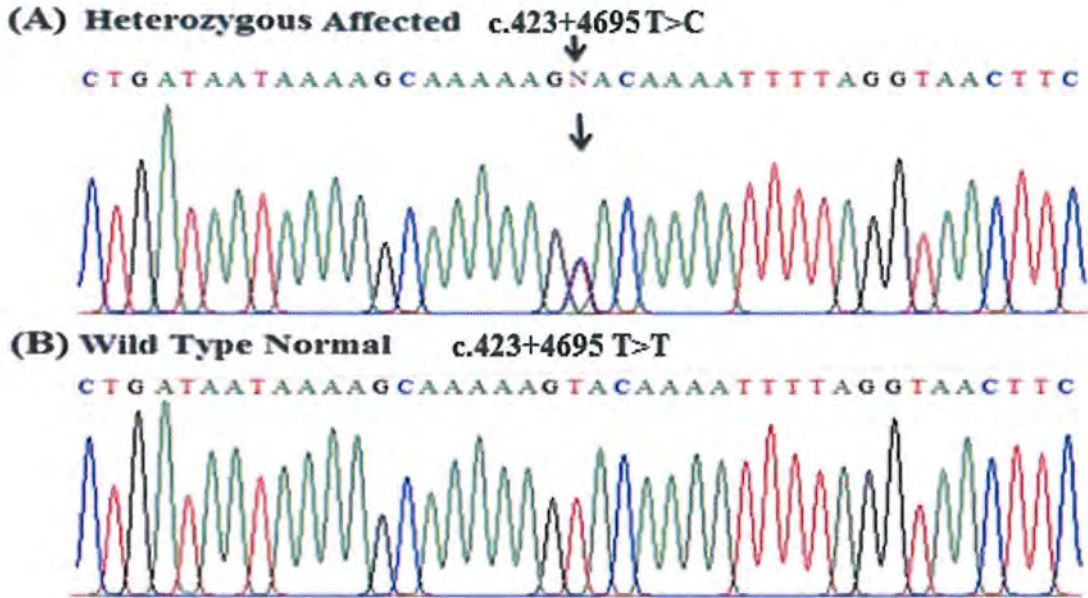
Figure 3.41 Panel (A) shows Sequencing chromatogram of *ZRS/SHH* with novel point mutation (c.423+4695T>C) within intron 182 T>C in heterozygous affected members, while panel B shows wild type with normal nucleotide sequence. Point of variation is presented with an arrow.

Chapter 4
Discussion

in hands. Affected members in all the four families did not show any other abnormality.

In three families (A, B, C) linkage was searched by typing microsatellite markers mapped in vicinity of the candidate genes. The genes tested included *GLI3* (7p13), *ZNF141* (4p16.3), *IQCE* (7p22), *GLI1* (12q13.3), *FAM92A* (8q22.13), *PITX1* (5q31.1), *SHH* (7q36.3) and *KIAA0825* (5q15). In addition, three other chromosomal loci (13q13.3-21.2, 13q21-32 and 19p13.1-13.2) were tested for linkage in the families as well. Analysis of the haplotypes, constructed from typed markers, revealed both affected and unaffected members were heterozygous for the gene alleles, therefore excluding the linkage in the families. This enhanced possibility of finding novel unknown genes responsible for the disorders in the three families.

In fourth family, direct Sanger sequencing of the genes *GLI3, SHH* and intron 5 of *LMBR1* (*ZRS/SHH*) revealed a novel heterozygous variant c.1034 + 182 T>C in the region of *ZRS/SHH*. Previously, Zhao *et al.* (2016) reported two pathogenic mutations (105C>G, 406A>G) in intron 5 of the *ZRS/SHH* in two Chinese families with TPT/PPD. These authors have identified enhancer sequences in intron 5 of *LMBR1*.Therefore, it is highly likely that any variant in the enhancer sequence for *SHH* perturb expression of the gene and result in malformation of limbs e.g. polydactyly.

In summary, three families (A, B, C) were failed to show linkage to already reported genes, predicting the involvement of other novel genes which are responsible for developing non-syndromic polydactyly. In order to search for the causative genes, recently developed technique exome sequencing will be one of the possible choices. The variant identified in the enhancer sequences in the intron of the *SHH* needed further characterization.

Chapter 5
References

References

Akarsu AN, Ozbas F, Kostakoglu N. (1997). Mapping of the second locus of postaxial polydactyly type A(PAP-A2) to chromosome 13q21-q32. (Abstract) Am J Hum Genet 61 (suppl.)

Anderson E, Peluso S, Lettice LA, Hill RE. (2012). Human limb abnormalities caused by disruption of hedgehog signaling. Trends Genet 28:364-373.

Barham G, Clarke, Nicholas MP (2008). Genetic regulation of embryological limb development with relation to congenital limb deformity in humans. J child Orthoped 2:1-9.

Barrow JR, Thomas KR, Boussadia-Zahui O, Moore R, Kemler R, Capecchi MR, McMahon AP (2003). Ectodermal Wnt3/β-catenin signaling is required for the establishment and maintenance of the apical ectodermal ridge. Genes Dev 17:394-409.

Bell J (1953). On syndactylies and its association with polydactyly. In: The Treasury of Human Inheritance. London: Cambridge University Press. V (II): 30-50.

Bell SM, Schreiner CM, Scott WJ (1998). The loss of ventral ectoderm identity correlates with the inability to form an AER in the legless hindlimb bud. Mech Develop 74:41-50.

Bénazet JD, Zeller R(2009). Vertebrate limb development: moving from classical morphogen gradients to an integrated 4-dimensional patterning system. Cold Spring HarbPerspBiol1:a001339.

Bennett RL, French KS, Resta RG, Doyle DL (2008). Standardized human pedigree nomenclature: update and assessment of the recommendations of the National Society of Genetic Counselors. J Gene Couns 17:424-433.

Bennett RL, Steinhaus KA, Uhrich SB, O'Sullivan CK, Resta RG, Lochner-Doyle D, Markel DS, Vincent V, Hamanishi J (1995). Recommendations for standardized human pedigree nomenclature. J Genet Couns 4:267-279.

Biesecker LG (2002). Polydactyly: how many disorders and how many genes? Am J Med Genet 112:279-283.

Biesecker, Leslie G (2011). Polydactyly: how many disorders and how many genes? 2010 update. DevDynam 240:931-942.

Bonafe L, CormierDaire V, Hall C, Lachman R, Mortier G, Mundlos S, Sillence D (2015). Nosology and classification of genetic skeletal disorders: 2015 revision. Am J Med Genet 167:2869-2892.

Bruneau BG, Nemer G, Schmitt JP, Charron F, Robitaille L, Caron S, Conner DA, Gessler M, Nemer M, Seidman CE, Seidman JG(2001). A murine model of Holt-Oram syndrome defines roles of the T-box transcription factor Tbx5 in cardiogenesis and disease. Cell 106:709-721.

Burger EB, Baas M, Hovius SE, Hoogeboom AJ, van Nieuwenhoven CA (2018). Preaxial polydactyly of the foot: Clinical and genetic implications for the orthopedic practice based on a literature review and 76 patients. ActaOrthopad 89:113-118.

Capdevila J, Belmonte JC (2001). Patterning mechanisms controlling vertebrate limb development. Ann Rev Cell Dev Biol 17:87-132.

Castilla E, Paz J, Mutchinick O, Muñoz E, Giorgiutti E, Gelman Z (1973). Polydactyly: a genetic study in South America. Am J Hum Genet 25:405.

Duboc V, Logan MP (2011). Pitx1 is necessary for normal initiation of hindlimb outgrowth through regulation of Tbx4 expression and shapes hindlimb morphologies via targeted growth control. Development 1:074153.

Fujioka H, Ariga T, Horiuchi K, Otsu M, Igawa H, Kawashima K, Yamamoto Y, Sugihara T, Sakiyama Y (2005). Molecular analysis of non-syndromic preaxial

polydactyly: preaxial polydactyly type IV and preaxial polydactyly type I. Clin Genet 67:429-433.

Furniss D, Critchley P, Giele H, Wilkie AO (2007). Nonsense-mediated decay and the molecular pathogenesis of mutations in SALL1 and GLI3. Am J Med Genet Part A 143(24):3150-60.

Furniss D, Kan SH, Taylor IB, Johnson D, Critchley PS, Giele HP, Wilkie AO (2009). Genetic screening of 202 individuals with congenital limb malformations and requiring reconstructive surgery. J Med Genet 46:730-735.

Gillessen KG, Majewski F (1991). Bilateral complete polysyndactyly (type IV Haas).Am J Hum Genet 38:29-31.

Graham T J, and Ress A M. (1998). Finger polydactyly. Hand Clin. 14, 49–64. Haas, S. L. (1940). Bilateral complete syndactylism of all fingers. Am. J. Surg 50, 363–366. doi: 10.1016/S0002-9610(40)90631-6

Haas SL (1940). Bilateral complete syndactylism of all fingers. The Am J Surg 50:363-366.

Hall BK (2018). Germ layers, the neural crest and emergent organization in development and evolution. Genesis 10:23103.

Horton WA (1993). Cartilage morphology.In Extracellular Matrix and Heritable Disorders of Connective Tissue.Alan R Liss New York 73–84.

Hovius SE (2018). A point mutation in the pre-ZRS disrupts sonic hedgehog expression in the limb bud and results in triphalangeal thumb–polysyndactyly syndrome. Genet Med 20:1405-1413.

Iimura T, Denans N, Pourquié O (2009). Establishment of Hox vertebral identities in the embryonic spine precursors: Current Topics. Dev Biol 88:201- 234.

Kini U, Nandeesh BN (2012). Physiology of bone formation, remodeling, and metabolism.InRadionuclide and hybrid bone imaging. Springer BerHeidelb 29-57.

Klopocki, E., Kähler, C., Foulds, N., Shah, H., Joseph, B., Vogel, H., et al. (2012). Deletions in PITX1 cause a spectrum of lower-limb malformations including mirror-image polydactyly. Eur. J. Hum. Genet. 20, 705–708. doi: 10.1038/ejhg. 2011.264

Kmita M, Duboule D (2003). Organizing axes in time and space; 25 years of colinear tinkering.Science 301:331-333.

Kobayashi T, Kronenberg HM (2014). Overview of skeletal development.InSkeletal Development and Repair. Humana Press Totowa NJ 3-12.

Kornak U, Mundlos S (2003). Genetic disorders of the skeleton: a developmental approach. Am J Hum Genet 73:447-474.

Krakow D, Rimoin DL (2010). The skeletal dysplasias. Genet Med 12:327.

Kondoh, S., Sugawara, H., Harada, N., Matsumoto, N., Ohashi, H., Sato, M., *et al.* (2002). A novel gene is disrupted at a 14q13 breakpoint of t (2; 14) in a patient with mirror-image polydactyly of hands and feet. J. Hum. Genet. 47, 136–139. doi: 10.1007/s100380200015

Kucheria K, Kenue RK, Taneja N (1981). An Indian family with postaxial polydactyly in four generations.Clin Genet 20:36-39.

Lange A and Müller G B. (2017). Polydactyly in development, inheritance, and evolution. Q. Rev. Biol. 92, 1–38. doi: 10.1086/690841

Kalsoom U, Klopocki E, Wasif N, Tariq M, Khan S, Hecht J, Krawitz P, Mundlos S, Ahmad W (2013). Whole exome sequencing identified a novel zinc-finger gene *ZNF141* associated with autosomal recessive postaxial polydactyly type A. J. Med. Genet. 50: 47-53.

Lee NK, Karsenty G (2008). Reciprocal regulation of bone and energy metabolism.Trends EndocrinolMetab 19:161-166.

Lefebvre V, Bhattaram P (2010). Vertebrate skeletogenesis: Current topics in developmental biology. Academic Press 90:291-317.

Lohan S, Spielmann M, Doelken SC, Flöttmann R, Muhammad F, Baig SM, Wajid M, Hülsemann W, Habenicht R, Kjaer KW, Patil SJ. (2014). Microduplications encompassing the Sonic hedgehog limb enhancer ZRS are associated with Haas-type polysyndactyly and Laurin-Sandrow syndrome. Clin Genet. 86(4):318-25.

Malik S.(2012) Syndactyly: phenotypes, genetics and current classification. Eur J Hum Genet. 20(8):817.

Malik S, Ullah S, Afzal M, Lal K, Haque S (2014). Clinical and descriptive genetic study of polydactyly: a Pakistani experience of 313 cases. Clin Genet 85:482-486.

Malik S (2014). Polydactyly: phenotypes, genetics and classification. Clin Genet 85:203-212.

Mariani FV, Martin GR (2003). Deciphering skeletal patterning: clues from the limb. Nature 423:319.

Martin RA, Jones M C and Jones K L. (1993). Mirror hands and feet with a distinct nasal defect, an autosomal dominant condition. Am J Med Genet 46, 129–131. doi: 10.1002/ajmg.1320460205

Mellin GW (1963). The frequency of birth defects. Birth Def 1-17.

Mundlos S, Horn D (2014). Limb Malformations: An atlas of genetic disorders of limb development.Springer.

Mundlos S, Olsen BR (1997). Heritable diseases of the skeleton. Part II: Molecular insights into skeletal development-matrix components and their homeostasis. FASEB J 11:227-233.

Nair SR, Varghese S, Kumar A and Jose RM (2001). A rare case of central polydactyly. Eur J Plast Surg. 24, 264–265. doi: 10.1007/s002380100249

Namba N (2010). Genetic basis for skeletal disease. Nosology and molecular classification of skeletal dysplasias.Clin Calcium 20:1159-1165.

Niswander Lee (2003). Pattern formation: old models out on a limb. Nat Rev Genet 4:133.

Olsen BR, Reginato AM, Wang W (2000). Bone development. Annual Rev Cell Dev Biol 16:191-220.

Palencia-Campos A, Ullah A, Nevado J, Yıldırım R, Unal E, Ciorraga M, Barruz P, Chico L, Piceci-Sparascio F, Guida V, De Luca A (2017). *GLI1* inactivation is associated with developmental phenotypes overlapping with Ellis–van Creveld syndrome. Hum Mol Genet 26:4556-71.

Perez-Lopez LM, la Iglesia DGD, Cabrera-Gonzalez M (2018). Radial Polydactyly. What's New?Curr Ped Rev 14:91-96.

Potuijt JW, Galjaard RJ, van der Spek PJ, van Nieuwenhoven CA, Ahituv N, Oberg KC, Hovius SE (2019). A multidisciplinary review of triphalangeal thumb.Eur J Hand Surg 44:59-68.

Radhakrishna U, Blouin JL, Mehenni H, Patel UC, Patel MN, Solanki JV, Antonarakis SE (1997). Mapping one form of autosomal dominant postaxial polydactyly type A to chromosome 7p15-q11.23 by linkage analysis.Am J Hum Genet 60:597.

Radhakrishna U, Bornholdt D, Scott HS, Patel UC, Rossier C, Engel H, et al. (1999). The phenotypic spectrum of GLI3 morphopathies includes autosomal dominant preaxial polydactyly type-IV and postaxial polydactyly type-A/B; No phenotype prediction from the position of GLI3 mutations. Am J Hum Genet 65:645-655.

Radhakrishna U, Wild A, Grzeschik KH, Antonarakis, Stylianos E (1997). Mutation in GLI3 in postaxial polydactyly type A. Nat Genet 17:269.

Rubin L, and Saunders JJW (1972). Ectodermal-mesodermal interactions in the growth of limb buds in the chick embryo: constancy and temporal limits of the ectodermal induction. DevBiol 28:94-112.

Sambrook J, Fritsch EF, Maniatis T (1989). Molecular cloning: a laboratory manual. Cold Spring Harbor Lab Press.

SaukaS,Tatjana, Bronner-Fraser M (2006). Development and evolution of the migratory neural crest: a gene regulatory perspective. Current Opinion in Genet Develop 16:360-366.

Saunders JJW (1948). The proximo-distal sequence of origin of the parts of the chick wing and the role of the ectoderm.J Exp Zoo 108:363-403.

SavarirayanR, Rimoin DL (2002). The skeletal dysplasias. Best practice and research.ClinEndocrinolMetabol 16:547-560.

Schrauwen I, Giese APJ, Aziz A, Lafont DT, Chakchouk I, Santos-Cortez R LP, Lee K, Acharya A, Khan, FS, University of Washington Center for Mendelian Genomics, Ullah A, Nickerson DA, Bamshad MJ, Ali G, Riazuddin S, Ansar M, Ahmad W, Ahmed ZM, Leal SM. (2018). *FAM92A* underlies nonsyndromic postaxial polydactyly in humans and an abnormal limb and digit skeletal phenotype in mice. J. Bone Miner. Res. 5Nov.

Summerbell D (1974).A quantitative analysis of the effect of excision of the AER from the chick limb-bud. Development 32:651-660.

Takeda S,Elefteriou F, Levasseur R, Liu X, Zhao L, Parker KL, Karsenty G (2002). Leptin regulates bone formation via the sympathetic nervous system. Cell. 111:305-317.

Temtamy SA, McKusick VA (1978).The genetics of hand malformations. Birth defects original article series: 14:364–439.

Thien HBD, Rüther U (1996). Cloning and sequence analysis of the murine Gli3 cDNA.BiochimBiophyActa BBA-Gene Struct Expr 1307:267-269.

Tickle C (2003). Patterning systems—from one end of the limb to the other. Develop Cell 4:449-458.

in hands. Affected members in all the four families did not show any other abnormality.

In three families (A, B, C) linkage was searched by typing microsatellite markers mapped in vicinity of the candidate genes. The genes tested included *GLI3* (7p13), *ZNF141* (4p16.3), *IQCE* (7p22), *GLI1* (12q13.3), *FAM92A* (8q22.13), *PITX1* (5q31.1), *SHH* (7q36.3) and *KIAA0825* (5q15). In addition, three other chromosomal loci (13q13.3-21.2, 13q21-32 and 19p13.1-13.2) were tested for linkage in the families as well. Analysis of the haplotypes, constructed from typed markers, revealed both affected and unaffected members were heterozygous for the gene alleles, therefore excluding the linkage in the families. This enhanced possibility of finding novel unknown genes responsible for the disorders in the three families.

In fourth family, direct Sanger sequencing of the genes *GLI3, SHH* and intron 5 of *LMBR1* (*ZRS/SHH*) revealed a novel heterozygous variant c.423+4695 T>C (182 T>C) in the region of *ZRS/SHH*. Previously, Zhao *et al.* (2016) reported two pathogenic mutations (105C>G, 406A>G) in intron 5 of the *ZRS/SHH* in two Chinese families with TPT/PPD. These authors have identified enhancer sequences in intron 5 of *LMBR1*.Therefore, it is highly likely that any variant in the enhancer sequence for *SHH* perturb expression of the gene and result in malformation of limbs e.g. polydactyly.

In summary, three families (A, B, C) were failed to show linkage to already reported genes, predicting the involvement of other novel genes which are responsible for developing non-syndromic polydactyly. In order to search for the causative genes, recently developed technique exome sequencing will be one of the possible choices. The variant identified in the enhancer sequences in the intron of the *SHH* needed further characterization.

Wagner EF, Karsenty G (2001). Genetic control of skeletal development.Curr Opin Genet Develop 11:527-532.

Warman ML, Cormier-Daire V, Hall C, Krakow D, Lachman R, LeMerrer M, Rimoin DL (2011). Nosology and classification of genetic skeletal disorders: 2010 revision. Am J Hum Genet A 155:943-968.

Winter RM, and Tickle C. (1993). Syndactylies and polydactylies: embryological overview and suggested classification. Eur J Hum Genet 1, 96–100. doi: 10. 1159/000472392

Yang Y, Drossopoulou G, Chuang PT, Duprez D, Marti E, Bumcrot D, Tickle C (1997). Relationship between dose, distance and time in Sonic Hedgehog-mediated regulation of anteroposterior polarity in the chick limb.Development 124:4393- 4404.

Yang Y, Niswander L (1995). Interaction between the signaling molecules WNT7a and SHH during vertebrate limb development: dorsal signals regulate anteroposterior patterning. Cell 80:939-947.

Zeller R, López-Ríos J, Zuniga A (2009). Vertebrate limb bud development: movingtowards integrative analysis of organogenesis. Nat Rev Genet 10:845-858.

Zemojtel T, Köhler S, Mackenroth L, Jäger M, Hecht J, Krawitz P,Spielmann M (2014). Effective diagnosis of genetic disease by computational phenotype analysis of the disease-associated genome.ScienTransl Med 6:123-252.

Zhao H, Tian Y, Breedveld G, Huang S, Zou Y, Jue Y, Lo WHY (2002). Postaxial polydactyly type A/B (PAP-A/B) is linked to chromosome 19p13.1-13.2 inaChinese kindred. Eur J Hum Genet 10:162-166.

Zhao, Ximeng, et al (2016). ZRS mutations in two Chinese Han families featuring triphalangeal thumbs and preaxial polydactyly. Zhonghua yi xue yi chuan xue za zhi Zhonghua yixue yichuanxue zazhi. Chin.J. Med Genet 33:281-285.

Zguricas J, Heus H, Morales-Peralta E, Breedveld G, Kuyt B, Mumcu EF, Bakker W, Akarsu N, Kay SP, Hovius SE, Heredero-Baute L (1999). Clinical and genetic studies on 12 preaxial polydactyly families and refinement of the localisation of the gene responsible to a 1.9 cM region on chromosome 7q36. J Med Genet. 36: (1):33-40.